Missouri S&T Library and Learning Resources

Scholars' Mine

Masters Theses

Student Theses and Dissertations

Spring 2018

Carbon black production, analyzing and characterization

Shadha Khalid Jebur

Follow this and additional works at: https://scholarsmine.mst.edu/masters_theses

 Part of the Chemical Engineering Commons

Department:

Recommended Citation

Jebur, Shadha Khalid, "Carbon black production, analyzing and characterization" (2018). *Masters Theses*. 7869.
https://scholarsmine.mst.edu/masters_theses/7869

This thesis is brought to you by Scholars' Mine, a service of the Missouri S&T Library and Learning Resources. This work is protected by U. S. Copyright Law. Unauthorized use including reproduction for redistribution requires the permission of the copyright holder. For more information, please contact scholarsmine@mst.edu.

CARBON BLACK PRODUCTION, ANALYZING AND CHARACTERIZATION

by

SHADHA KHALID JEBUR

A THESIS

Presented to the Faculty of the Graduate School of the

MISSOURI UNIVERSITY OF SCIENCE AND TECHNOLOGY

In Partial Fulfillment of the Requirements for the Degree

MASTER OF SCIENCE IN CHEMICAL ENGINEERING

2018

Approved by

Dr. Joseph Smith, Advisor
Dr. Douglas Ludlow
Dr. Peter Ryan

Copyright 2018

Shadha Khalid Jebur

All Rights Reserved

ABSTRACT

Carbon black (CB) plays a significant function in the development of the electrical and mechanical properties of high performance for a tough elastic polymeric substance such as rubber materials. Thus, CB is widely used to manufacture a massive number of products such as reinforcing and pigment phase in automobile tires due to its high ability to increase tire life by reducing the thermal damage. This material is also used in belts, hoses, and other non-tire rubber goods. Before use in valuable materials. CB should first be analyzed and characterized by different instruments to obtain its mechanical properties. A new thermal black process by using electrical heating system has been used in this work. Which will produce a new grade of the CB with the high surface area for use in tire manufacturing.

This thesis demonstrates that the production of carbon black was characterized by transmission electron microscopy (SEM), X-ray diffraction (XRD), and Brunauer-Emmett-Teller (BET) measurements. These techniques have been used for the solid samples (powder). Additionally, Fourier-transform infrared spectroscopy (FTIR) and gas chromatography (GC) have been utilized for gas samples.

ACKNOWLEDGMENTS

Thankful to God (ALLAH), prophet (Mohammed) and his holy family, Prophet Jesus Christ, his holy mom miss Maria. This thesis would not have been complete without the support of Dr. Joseph Smith. My deep thanks to Dr. Smith for his endless tolerance and direction at each progression of this work. My thankful to Dr. Douglas Ludlow and Dr. Dwindle Ryan for willing to be on my committee advisory group and their kindness. I should thank my lab mates: Haider, Manohar, Anand, Vivek, Aso, Jia, Han, Haider Alhamedi and Jeremy. I am appreciative to Dr. Darrell Ownby, Dean, Dawn and Emily for their assistance. I would like to thank Monolith Materials Inc. for their financial support. Deep acknowledgment to Dr. Nathan Leigh and Mr. Satterfield for GC and FTIR training and their efforts. Thankful to Dr. Jeremy Watts and Devin Mc Millen for BET training and their generosity for using their lab anytime. I would like to thank Dr. Eric Bohannan to help us with XRD analysis. I present my work to the spirit of my dear father, to my dear mother, and my second father Mr. Salim Sabri that they were continually being with me through their hearts and prayers. Acknowledgment to my husband, Dr. Laith Sabri, for his help. Thankful to my sister Fatima for her inspiration, effective support for me. Thanks to admired Brother Mohammed for all help and support. To instructor and Brother Dr. Abbas Sultan, there are no words to describe your character; thank you for your support and responsibility. To my best friends Majeda, Mrs. Ammal, Dr. Naven Ali and Daad, my gratitude for your support and prayers. To Mrs. Cathy Cassidy, Dr. Cassidy, and Sierra, thank you for making me feel at home, for all the fun times together in Rolla, and for your support and responsibility for my family.

TABLE OF CONTENTS

LIST OF ILLUSTRATIONS

Page

LIST OF TABLES

Page

1. INTRODUCTION

Carbon black (CB) is a term that mentions to a group of industrial materials products including furnace, thermal and acetylene blacks. They basically contain carbon in a form close to spherical particles of colloidal size combined into particle combinations and are achieved by thermal decomposition of hydrocarbons and the partial combustion. Therefore, CB shows a major role in the enhancement of the rubber materials in terms of mechanical and electrical properties. The potential of the reinforcing mostly refers to two things: first, the formation of the filler network physically in a bonded flexible, and second, strong filler by polymer couplings. The effects of both parameters refer to a big surface activity and specific surface of the filler particles. To this point, the structure and formation of the network in the CB and the mechanical response work in terms of analyzing and characterization (Alcántara et al. 2001; J. B. Donnet, R. C. Bansal 1993; Knoblauch et al. 2011; Kraus 1978; Lohmann, Macfarlane, and Gschwend 2005; Chen et al. 2014; James E. Mark 2007; Martínez, Murillo, and García 2013).

In previous centuries, CB was used by the Indians and Chinese. It has been used as a pigment in the black ink. After that, the carbon was commonly used as a filler in paints, elastomers, and plastics to adjust the electrical, the optical properties and mechanics of the materials in which they are scattered, thus setting their implementation in a specific market segment (Anonymous 2011; DuBay and Fuldner 2017; Kuhlbusch 1998; Luengo, Treuillet, and Gomez 2015; Avrom I. Medalia 1986).

Unique properties have imparted when CB is compounded with plastics, such as UV protection, electrical behavior, or the range of darkness (jets). Around 90% of the worldwide production of CB is utilized in tire manufacturing where the CB develops tear

strength, perfect modulus and wear analysis of the tires (Borchard et al. 2014; Probst and Grivei 2002a).

CB is a remarkable pigment for use in xerographic toners as it help maintain a suitable level of electric charge on the toner which essential for proper operation of the electrographic over 2000 printers.

Total manufacture for CB was around 8,100,000 metric tons. After that the amount of CB consumption estimated globally in 2015 was more than 13.3 million tons and priced at $13.9 billion, and it is predicted to reach 14 million tons at $14.6 billion in 2016. Advance prediction is to preserve 5.8% between 2016 and 2022 to reach 19.4 million tons, which is equivalent to $20.6 billion in 2022.

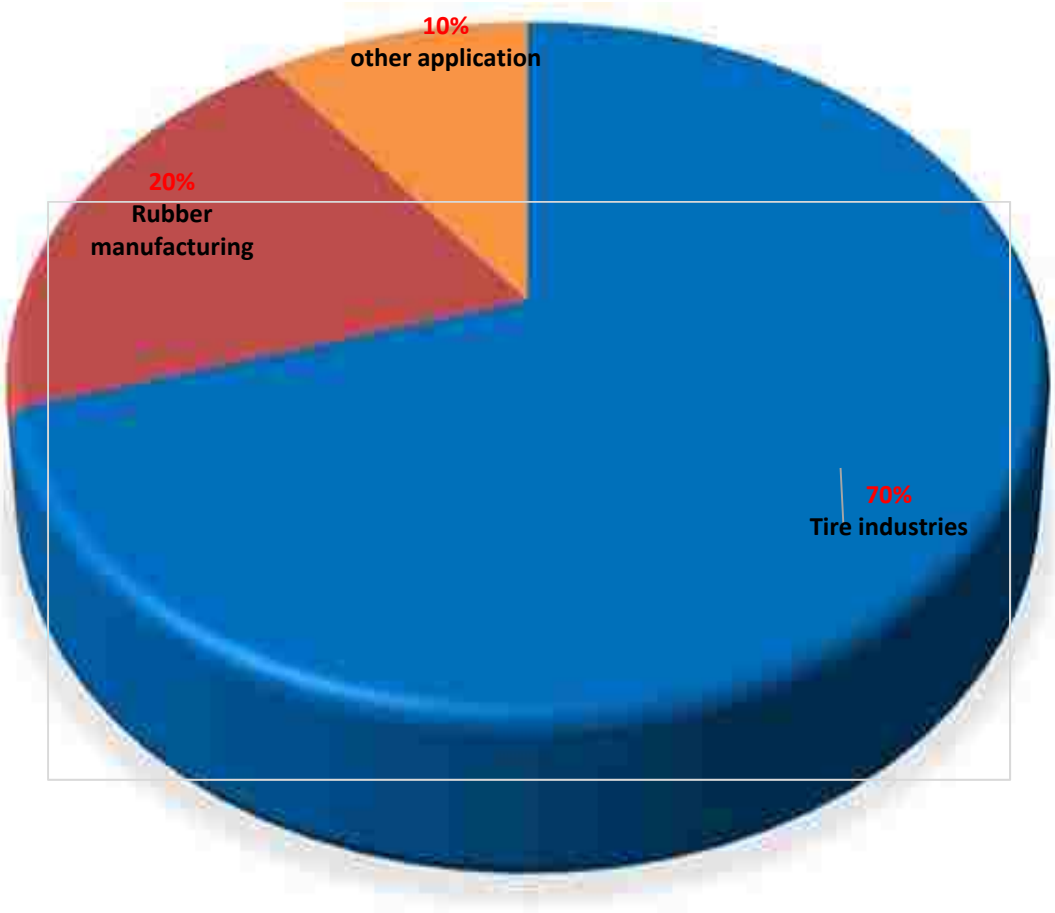

Figure 1.1. Global Carbone Black Demand by Application until 2018

The general use for CB is now a days is (70%) as shown in Figure 1.1, where the majority (70%) of use is as a reinforcing phase and pigment in automobile tires. likewise, the behavior of heat away from the tread and belt area of the tire by the CB supports increases tire life by reducing thermal damage (A. Tomlinson E. Karakosta, M. Oakey, T.N. Danks, D.M. Heyes, S.E. Taylor et al. 2000; Anonymous 2011; Borchard et al. 2014; Knoblauch et al. 2011; Szozda 1996). Some absorbent materials use the particles of the CB in radar for the decrease of cross-section of the radar in aircraft, in laser printer toner and photocopiers, and in other paints and inks.

The high strength of the paint and the carbon black stabilization also has use in the coloring of films and resins. Other utilization, which around 20%, is in hoses, belts, and other non-rubber materials, where it is mostly used as a pigment in inks, plastics, and coatings, as shown in Figure 1.2 (Dong et al. 2017; Fan and Zhang 2008; Knoblauch et al. 2011; Major et al. 2010). Additionally, CB has been greatly used in packaging for food and beverage around the world as a phase of color pigment. It is used in milk bottles in the United States, South Africa, and parts of Europe, and Asia, and in New Zealand it has been used in items like microwavable meat trays and meal trays.

There are rigorous guidelines available and in place to ensure the employees who work in CB industries are not in a working environment where they are at risk of inhaling unsafe doses of CB in its raw form (A. Tomlinson E. Karakosta, M. Oakey, T.N. Danks, D.M. Heyes, S.E. Taylor et al. 2000; Dons et al. 2012; Fowles 2007; Miao et al. 2013; Moulin et al. 2017; Payne and Whittaker 1970; Sorahan et al. 2001; M.-J. Wang et al. 2003).

Figure 1.2. Carbon Black Uses

1.1 CARBON BLACK PROPERTIES

The complicated structure of carbon black observed under an electron microscope shows that they have, mostly spherical particles fused together. The spherical particles are different sizes. Particles connected as a chain are called a "structure." Several practical assemblies such as the group of the carboxyl or hydroxyl are found in the CB surface. The name "surface chemistry" is given for their composition or amount. Surface chemistry particle size and structure are the simple carbon black properties. These properties are main parameters for carbon black and have a big effect on the properties of the particle such as dispensability and blackness when they are mixed with inks, paints, or resins (Kwon, Kim, and Rhee 2013; Samaržija-Jovanović et al. 2009). Therefore, it can be defined the carbon black generally as a very fine particulate aggregates of possessing of the carbon a formless quasi-graphitic molecular structure. The greatest areas of differences between a furnace black and thermal black are the size of the particle and the formula of the structure. Most carbon blacks are assigned and classified a number of the grade established on the surface area and the measurements of the structure (Kwon, Kim, and Rhee 2013; Moulin et al. 2017; Poudel and Qiao 2014; Tang et al. 2015).

1.1.1. Sieve Residue. Sieve residue indicate to contaminants as a non-dispersible for example refractory particles, coke, metal oxides and water-soluble salts, and it is defined as a carbon black percentage by weight. The sieves in sixty and 325 Mesh are utilized for this test. The gravel resulting could cause shortcomings and might impact the performance and manifestation of some plastic and rubber products. The 325 mesh grit is also tested for magnetic content (Bossuyt, Six, and Hendrix 2006; Rating 2000). The concept of carbon black as an "aggregate" is more suitable to describe the chaining and clustering of CB particles. Hess and Ford (79) referred to aggregates in terms of the discrete

units of CB that exist in elastomer vulcanizes. However, this terminology was not widely used until the work of Medalia (Köchling et al. 1985; A. I. Medalia 1978; A. I. Medalia and Heckman 1969). By viewing carbon black through high-resolution electron microscope characterization, Burgess et al. [81] found that the aggregate of the carbon black as a "paracrystalline unit".

The carbon black particles were known as the field or area of the layer orientation for graphitic rotation. While this terminology was described as the true nature of CB, it was not exceedingly reasonable. This also applies to the term "nodule" which was used to describe the CB particles. In present day, the terms “aggregate” and “particle” are used as the main descriptors of carbon black morphology. The separate, colloidal rigid structure for the aggregate of the CB which is the lowest dispersible unit is composed of comprehensively coalesced particles.

The carbon blacks particles fusion is made up of all electrons. The structural properties and the shape of the distributive aggregate in nature; such as the size of the aggregate grades and the particle size. They occasionally differ through a broad range within and between the agglomerate. An agglomerate is also confused with an aggregate and is actually comprised of a large number of aggregates that are physically held together as opposed to the graphitic structure which links the continuous particles in aggregates. The important in particle size and its distribution is most likely CB in terms of physical properties and end-use applications, even though particles do not exist as discrete entities except for thermal blacks. Therefore, the methods employed to measure particle size directly and indirectly will be described first, followed by those for surface area, porosity and aggregate size and shape.

1.1.2. Particle Size. The size of CB particles particularly the diameter of the particle when it has a spherical shape as shown in Figure 1.3, is considered as an essential characteristic that largely effects dispensability and blackness when mixed with resins or other vehicles. Generally, the minimal size particle becomes maximal blackness of carbon black. Scuttle, however, becomes hard due to an increase in coagulation force. The size of the particle of the CB distributions, when the electron microscope remains accurate means of the measuring. The first extensive measurements were by Ladd et. al. (1942), for commercial grade carbon blacks. They measured manually on suitably enlarged micrographs. Typically, based on a high frequency discharge, the dispersions used in these early studies scattered the CB onto thin plastic films of polyvinyl formal or nitrocellulose (Jean-Baptiste Donnet, Bansal, and Meng-Jiao Wang 1993).

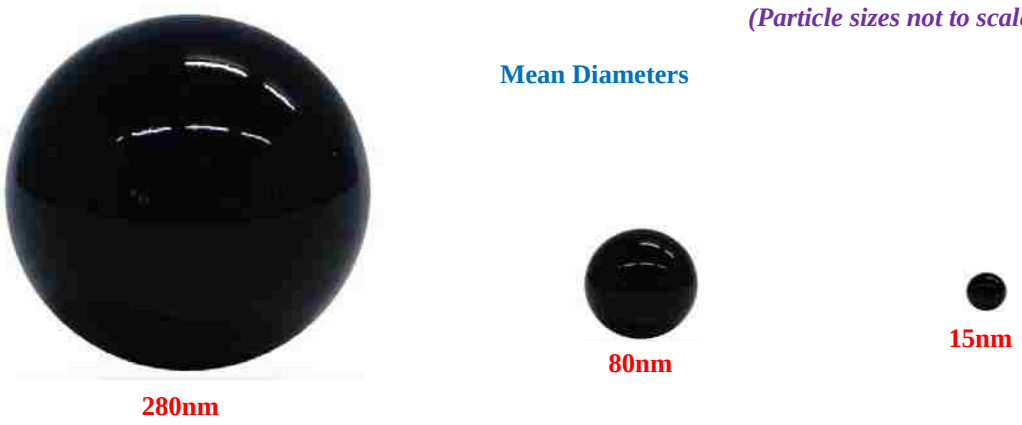

Figure 1.3. Carbon Black Particle Size Comparison

Endter, F. and Gebauer (1956) made main advance by improving a semiautomatic measuring device, which was later marketed by the Zeiss Optical Co. This instrument utilizes a variable light spot to measure the particle diameters on micrographs, and the values are recorded automatically. Schubert et al. (1969) described the application of the Zeiss Particle Size Analyzer for CB particle size measurements along with procedures for estimating particle size from micrographs. It was later found that the discharge method

actually altered some of the CB particles through oxidation or partial graphitization (Syvitski J. P. M. 1991; Syvitski, LeBlanc, and Asprey 1991).

1.1.3. Structure. Similar to particle size, the structure size also impacts the dispensability and blackness of carbon black, as shown in Figure 1.4. Commonly, the increase in size of the structure increases dispensability, through it lowers blackness. CB with a larger structure or construction displays excellent conductivity (Black, Pearls, and Spectra 1996; J. B. Donnet, R. C. Bansal 1993).

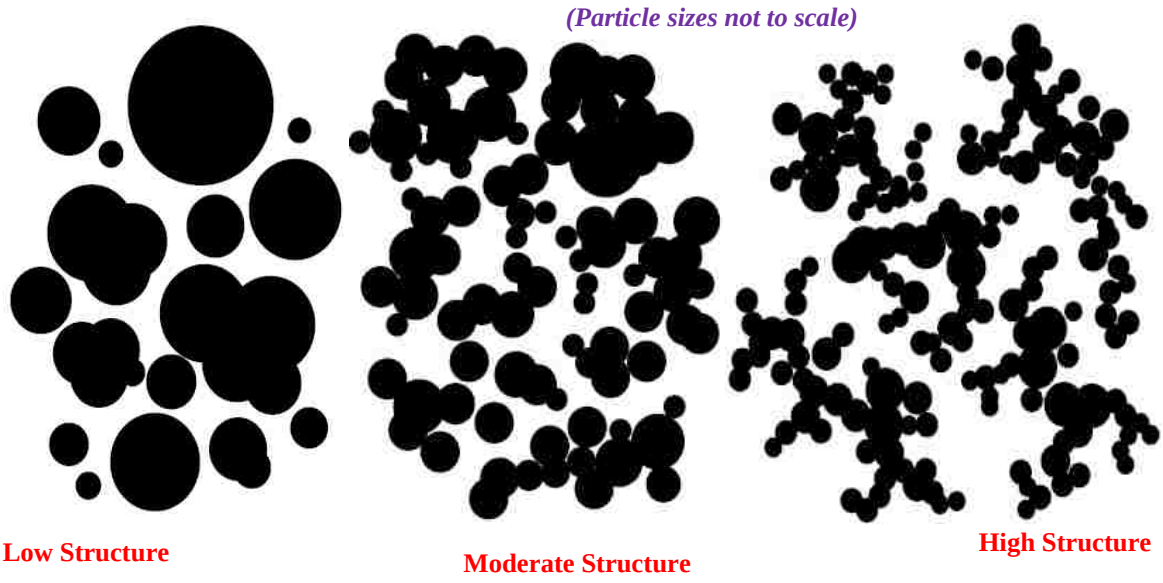

Figure 1.4. Carbon Black Structure

1.1.4. Surface Area. The surface area plays a substantial role in CB grade production and classification. For non-porous CBs, the values exhibit an overall inverse correlation with particle size. However, it is inadvisable to try to forecast either property from the other. Furthermore, surface areas provide no distributional information. Several measures are accessible for obtaining the surface area and usually involve the specified adsorption molecules on the CB surface.

Three of the most widely used adsorption methods are based on nitrogen (ASTM 1990), cetyltrimethyl ammonium bromide (ASTM 1990), and iodine (ASTM 1990). Other gaseous adsorption techniques are also available. The surface areas derived from of the above methods can be affected in different ways by the amount and type of porosity, as well as the chemical nature of the surface of the CB being analyzed.

It is important, therefore, to keep these possible effects in mind when interpreting the surface area data from each specific test (Liang 2004).

One of the main measurements to determine of CB particle size is the surface area. Two methods have been used to obtain the surface area:

Measuring the iodine adsorption amount (mg/g-carbon) which could be adsorbed on the surface CB, and by using the nitrogen, which can measure the adsorbed amount on the surface area which gives the mass of CB.

All previous methods have the perfect behavior of most grades in the rubber of the blacks furnace, however, toluene extract on the thermal blacks surface interferes with the aquatic iodine-potassium method of the adsorption iodine technique, and the surface area measurement by nitrogen makes it analyze improperly. Consequently, the American Society for Testing and Materials (ASTM) does not recommend the adsorption of iodine for measuring surface area.

The mean diameters are 240 - 320 nm for largest particle size of thermal black in any CB and hence 7-11 m^2/g is lowest surface area. In disparity, particle sizes in furnace black are around three to twenty times less in mean diameters (15 - 80 nm) on the condition surface areas from 27 - 145 m2/g. The thermal black in particle size is shown in comparison with the minimum and maximum particle size of furnace blacks in Figure 1.5.

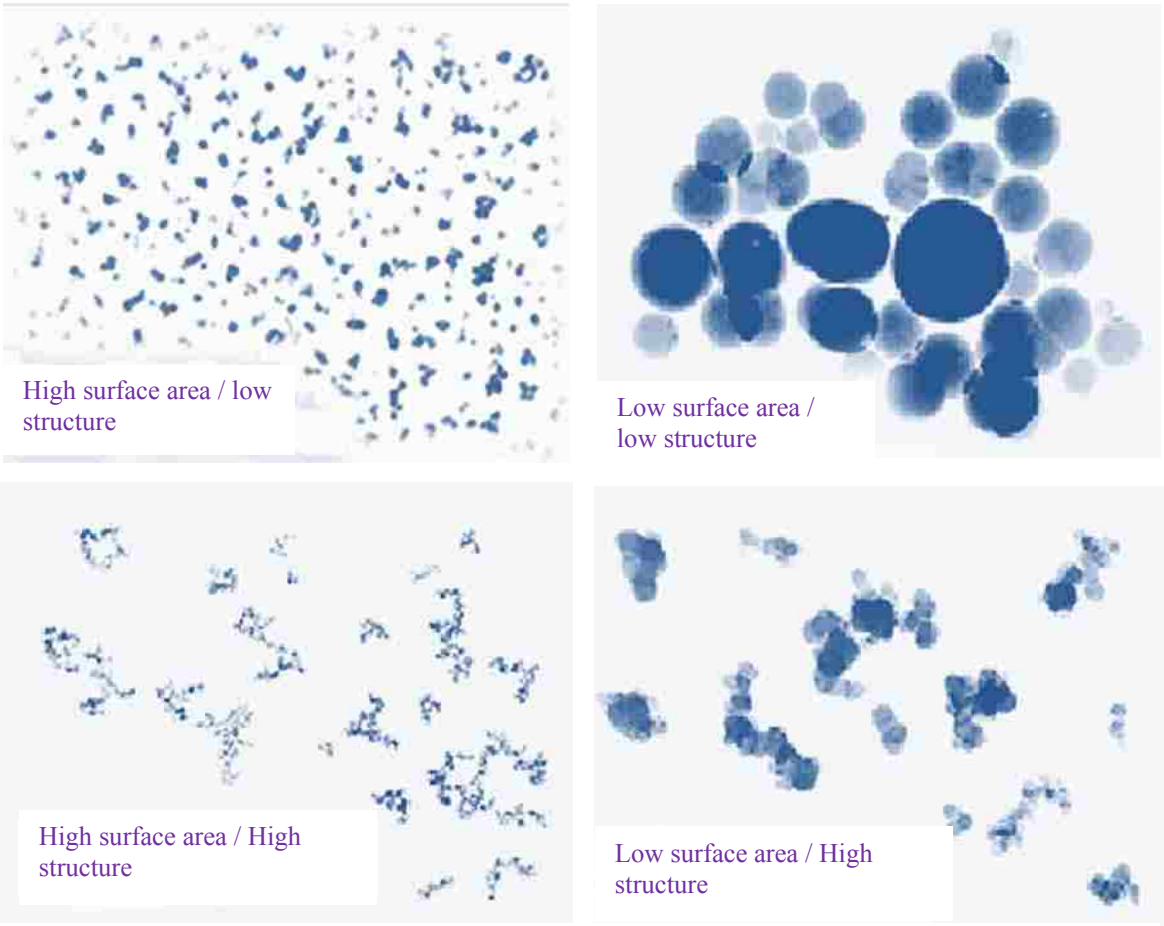

Figure 1.5. Comparison of surface area at different particles structures *(http://www.cabotcorp.com/solutions/applications/industrial-rubber-products/dispersion)*

As a results, the BET methods have found great utility because they are simple to use and can generally model the five basic isotherms normally observed and yield the most accurate results for surface area determination compared to other adsorption theories (Borah et al. 2008; Probst and Grivei 2002b; M.-J. Wang et al. 2003).

1.1.5. Surface Chemistry. Several practical groups exist on the surface of the CB. The affinity of CB with paint or inks polishes changes depending on the kind and the quantity of the practical groups. In large amount and given with oxidation treatment, the

hydroxyl group in CB which has greater attraction to print inks or varnishes, shows excellent dispensability.

1.1.6. Porosity. The characterization porosity in carbon blacks is essential from a theoretical and practical standpoint. The porosity can affect the measurements of the surface area and for other tests. It can also impact certain applications and properties by increasing the effective loading of the CB. Theoretically, porosity is also necessary in the microstructure understanding and formation of CBs. Numerous books are available that contain information on the analysis of porosity in materials (Geschke 2007; Pierson 1993).

The CBs porosities can be divided into two types, open and closed porosity. Open porosity can be in the form of small pores of the order of nanometers of an undefined shape on the surface which may or may not provide access to internal voids. If the internal voids are not accessible to the surface, they represent closed porosity. Internal porosity may occur as a result of oxidative hollowing out of the centers of individual particles within an aggregate (Golberg 1985; J. B. Donnet, R. C. Bansal 1993; L. Wang et al. 2011).

This type of porosity is available to small gas molecules and will affect surface area measurements in two methods: first, additional internal surface is measured, and, second, the total number of aggregates per unit weight increases from the oxidative carbon removal. A second type of internal porosity exists in the more disordered core of the CB particles, is generally closed to the surface, particularly after heat treatment of the CB at high temperatures. The primary methods for determining the degree of porosity in carbon blacks are based on density and gas adsorption techniques. Mercury porosimetry is not considered a viable method, especially for small particle size carbon blacks, because the very high pressures that are required can result in compression of the sample (Biscoe and Warren 1942; Carbon and Change 2010; Golberg 1985; J. B. Donnet, R. C. Bansal 1993; Loutfy

1986). The determination of the density can be done in several ways and will be discussed in next sections (J. B. Donnet, R. C. Bansal 1993).

1.1.7. Density. The density of CB and other materials can have a number of different meanings. Values based on microcrystallinity are usually accepted as the true material density. Other commonly used procedures are based on pycnometer measurements using helium or different liquids. In addition, there is "bulk density" which typically refers to the packing density of the CB as it is supplied for commercial use. All of these various aspects of density are important and certain measurements, when combined, also provide information pertaining to the type of porosity (open vs. close that exists in a carbon black X-ray Measurements Densities based on X-ray diffraction are derived from the atomic spacing within the unit cell of a material and are, therefore, independent of porosity and other effects. X-ray densities form a broad range of carbon blacks along with graphite. All of the carbon blacks were analyzed before and after heating in an inert atmosphere at temperatures ranging up to 2500 or 2800°C.

1.1.8. Aggregate Size. Aggregates represent the true primary units of CB. However, unlike particle size which is not affected by mechanical handling, aggregate size is system dependent. High shear mixing in polymeric systems causes significant aggregate breakdown relative to the dry state.

1.1.9. Aggregate Shape. The aggregates of the CB is differ in form from the specific spherical particles that are established in thermal CBs to the extra grouped and rubbery types that are common in all other grades (Gómez-Serrano, González-García, and González-Martín 2001). The presence of these more complex shapes creates internal voids within any given bulk sampling of carbon black which is much greater than those that occur in a simple packing of spheres. It is not surprising then that the most commonly used methods for CB measurement "structure" have been based on internal void volume using volumetric or absorptive measurements under specific pressure conditions (Kim and Jeong 2005).

The absorptive capacity of a carbon black for liquids is predominantly related to aggregate shape (i.e., highly open aggregates). The structure of the branched is able to absorb more vehicle together internally and in the voids between them and other aggregates than close individual spheres or packed particle aggregations. In the latter instance such as thermal blacks, internal aggregate occlusion of vehicle is essentially zero. High absorption can be achieved with either large particle size (very large voids) or small particle size (greater number of smaller voids).

A method for measuring the oil absorption of CB was described by Sweitzer and Goodrich in 1944 (Sweitzer and Goodrich 1944). Linseed oil was added dropwise to a 1 g sample of CB and mixed with a spatula using moderate pressure. During this process tiny pellets are formed that gradually increase in size and diminish in number as additional oil is added. An end point is reached when a single ball of stiff paste is formed, indicating that the voids within the CB have been filled with oil. The higher the oil absorption per unit weight of black, the greater the extent of the aggregate structure. Absorption occurs both within the aggregate branches and between contacting aggregates in a 3-dimensional network (J. B. Donnet, R. C. Bansal 1993).

1.1.10. Electronic Properties. Electrical resistivity in the CB is a semiconductor and its use in many product electrical conductivity (or its inverse, resistivity) is important (Galli 2010). Many researchers have reviewed the electrical properties of CB in polymeric composites. While this is not of this particular chapter, some of the information presented by these authors is also pertinent to electrical conduction in the dry state. Medalia (Avrom I. Medalia 1986) has summarized the most important mechanisms of electrical conductivity in CB composites, which include: electron tunneling emission, dielectric breakdown and internal field, capacitance chains, and graphitic conduction (thorough chains). Graphitic conduction contacting CB aggregates is most

prevalent at high CB loadings (J. B. Donnet, R. C. Bansal 1993; James E. Mark 2007; Snowdon, Mohanty, and Misra 2014).

1.1.11. Thermal Conductivity. The thermal conductivity of a material is typically derived at steady state from the quantity of heat flow per unit area or length across a temperature gradient (J. B. Donnet, R. C. Bansal 1993; James E. Mark 2007).

1.2. MANUFACTURING PROCESSES

CB is produced by combusting oil or gas with a great deal of oxygen inside large furnaces. The furnace walls lined with bricks become very hot because the oxygen and oil combust. By varying the amount of oil and air, the internal temperature of the furnace can be altered, which permits manipulation of the particle size and particle connections of the carbon black being produced. The time required to produce CB from oil is so short that it cannot be observed by the human eye.

The large industrial scale, in general for carbon blacks manufacturing consists of the following sections: storage facilities for feedstocks, carbon black production units, equipment for the separation of CB from the process off. gas (tail gas), final processing of the carbon black, and finally storage facilities for the end product, utilization of waste gases. The individual sections are interconnected by transport and conveying facilities which are completely closed systems in modern carbon black plants avoiding the release of carbon black dust into the surroundings. Industrial carbon blacks constitute no health hazard (32). However because of its considerable coloring strength the product is regarded as a nuisance dust. Therefore, emission controls are an important aspect of carbon black production.

1.2.1. Classification of Carbon Black Manufacturing Processes. It is crucial, from the chemical perspective, to classify CB production processes into two main groups of *incomplete combustion* and *thermal decomposition of hydrocarbons*, depending upon the absence or occurrence of oxygen. The process of incomplete combustion, termed thermal oxidative decomposition, is by far the most important. In terms of quantity, the second process i.e., the thermal decomposition of hydrocarbons in the absence of oxygen, plays only a very limited role. In practice, the methods used to produce CB can be classified according to the criteria shown in Table 1 (J. B. Donnet, R. C. Bansal 1993; Zielinski and Kijenski 2005).

Table 1. Kinds of Carbon Black Manufacturing Processes

Manufacturing process	Raw material	Manufacturing method	Explanation
Incomplete combustion	Aromatic hydrocarbon oil	Oil furnace	This is currently the most common method
	Mineral/vegetable oils	Lampblack	Oldest industrial method
	Natural gas	Channel	Flames contact the lower surface of a channel (an H-shaped steel beam)
		Gas furnace	Useful for fine-particle carbon black
Thermal decomposition	Acetylene	Acetylene decomposition	As this is a heat-generation reaction, continuous production is possible
	Natural gas	Thermal	Combustion and thermal decomposition are repeated in cycles

Figure 1.6 shows the steps of CB manufacture as an individual process. The heart of the process is the CB production unit (Reactor or Apparatus) which, depending on the process, may consist of reactor(s) or apparatus.

The initial product of the unit is a mixture of process gas and CB suspended in the form of an aerosol. This aerosol is cooled and directed into collecting systems (Filter), where the solids are separated from the process gas. The CB thus obtained has a fluffy appearance, hence the designation “fluffy black". Due to its low bulk density and its tendency to dust, the black cannot be handled in this form and, therefore, must to be subjected to some form of densification (Wet Pelletization, Dry pelletization, Densification).

The fluffy black is either densified to powder black (Densification) or pelletized and, depending on the pelletizing process, dry or wet wet-pelletized CB is obtained. The CB is then conveyed to the storage and packaging sections (Final product silo, Packaging of pellets, Packaging of powder).

Powder black is always packed in bags (Packaging of powder), whereas pelletized black is shipped either in bags, usually shrunk or stretch-wrapped on pallets (Packaging of pellets, Packaging of powder, Storage of bags, Shipment of bags), or as bulk or semibulk material (Bulk shipment) in road or rail tankers or in containers.

1.2.1.1. Furnace black method. The process of the furnace black is used for the production of the CB. This method is the most modern method for CB manufacturing. In this method, the continual thermal decomposition generates heat by using the combustion of air and fuel. The process is continuous, and is operated in closed reactors where highly turbulent flows prevail due to high flow velocities.

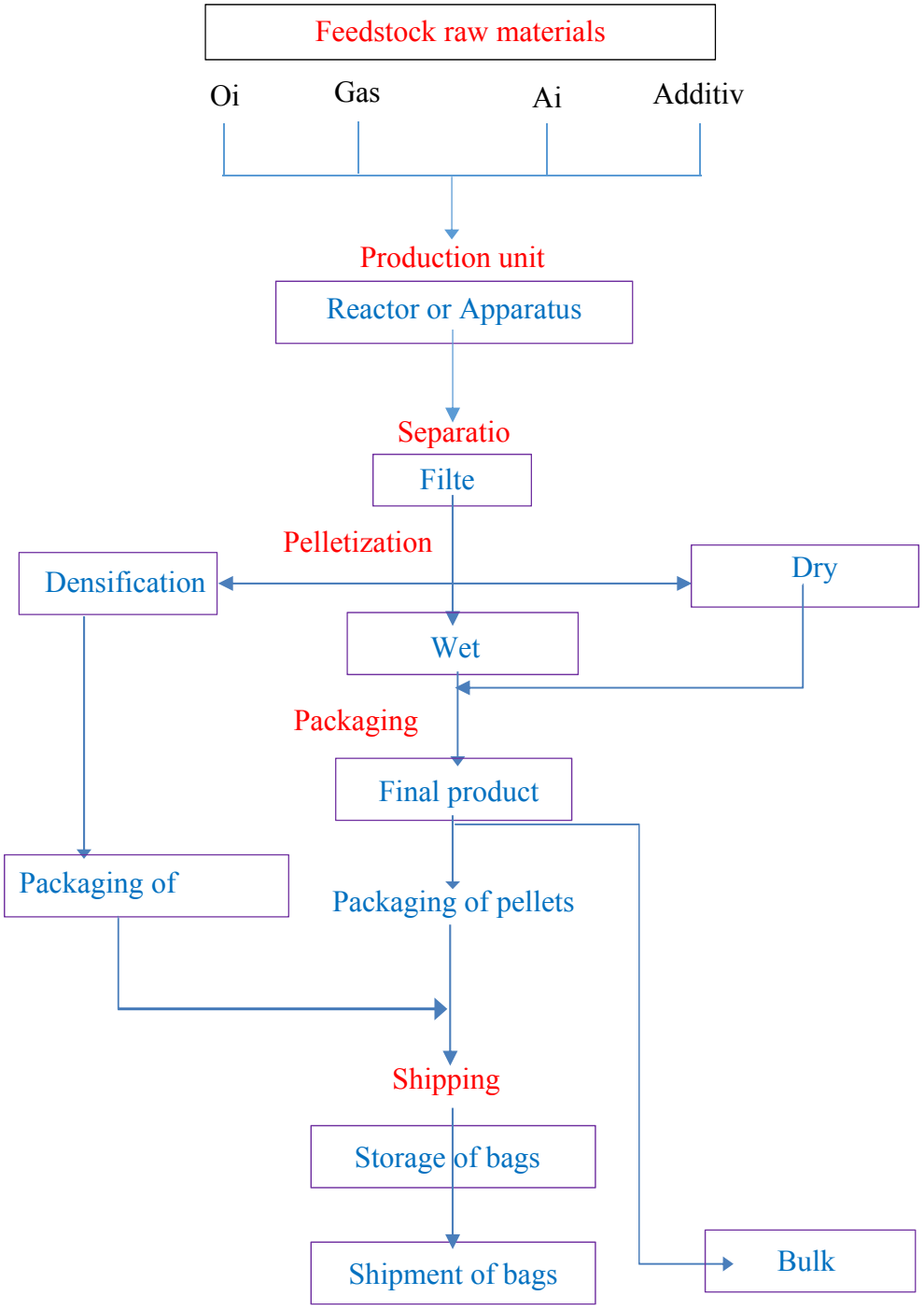

Figure 1.6. Schematic diagram of the individual process steps in a carbon black production unit

The section of the reaction is lined with a material that is heat-resistant. Hot fuel (oil) and air are introduced into this reaction unit to bear the complete combustion that reaches the temperature of 1300ºC. And when the atmospheric high-temperature was formed, the oil which is the feedstock to the reaction section is continuously atomized for thermal decomposition. The gas at high-temperature with the formed CB moves downstream in the reactor and is atomized with water to readily lower its temperature to more than 1000 degrees, which will stop the reaction.

The period among the formation of the CB and the end of the reaction are very short generally about a few milliseconds to two seconds. Through this short time of the process reaction, adjustments made to the shape of the reactor and conditions of the manufacturing, such as the temperature of the reaction and the time of the reaction which make the manufacture of the CB possible with structures (particle bonds) and various particle sizes. This process uses the principle of oxidative decomposition as shown in Figure 1.7.

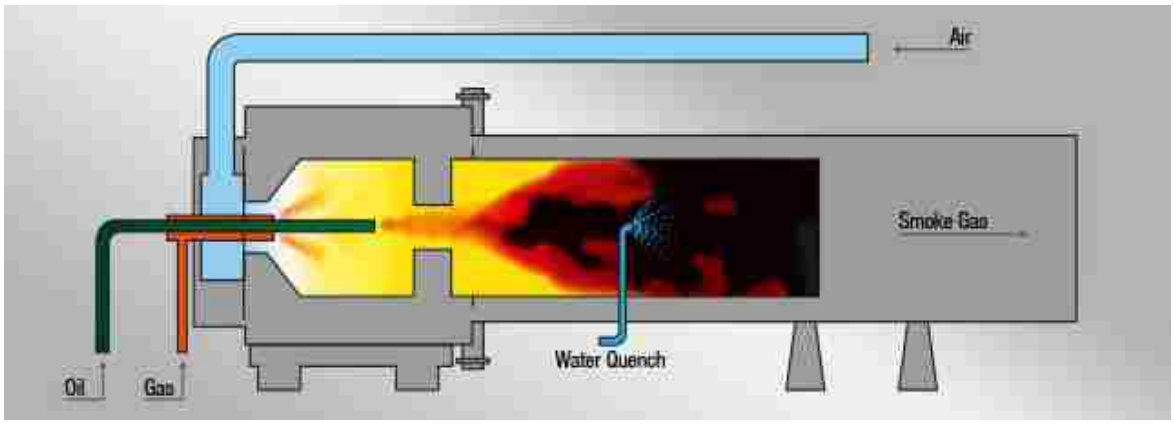

Figure 1.7. Internal diagram for the furnace black process (J. B. Donnet, R. C. Bansal 1993)(https://pentacarbon.de/wiki/)

1.2.1.2. Lampblack process. Black carbon production by the lampblack process is one of the oldest manufacturing processes. Since the ancient past, huge carbon black quantities have been required for the preparation of inks, but also of paints for mural paintings. Mainly, these were produced by the lampblack process. The Roman architect Vitruvius already described the preparation of lampblack from the resin of pine trees. The major feature of this operating system, such as heating of the limited air supply and recovery of the carbon black in depositing chambers, remained unchanged for centuries.

The lampblack process belongs to the processes of thermal oxidative decomposition and is characterized by great simplicity. The only feedstock required is an aromatic oil mainly based on coal tar. The lampblack apparatus, shown in Figure 1.8, consists of a flat cast-iron pan that contains the liquid feedstock, the level of which has to be kept as constant as possible. A refractory-lined hood is installed above the pan in such a way that a ring-shaped gap is left between the edge of the pan and the hood. The process air is fed into the system through this gap. A water-cooled tube that is connected to the hood cools the carbon black smoke.

The carbon black is then separated in filters and pelletized as in the furnace black process. The lampblack process has only one variable input parameter: the process air. The size of the gap and the vacuum generated by the suction created by the filter fan determine the amount of air drawn in and hence the reaction temperature.

At increased air rates, a greater portion of the feedstock is burned, leading to higher temperatures. These result in the formation of smaller primary particles and higher specific surface areas. However, the process is not very flexible with a given set of equipment. For fine-particle

blacks, the pans have to be small, and inversely, large-particle blacks require feedstock pans with large diameters.

The input of air from the periphery creates areas where different conditions prevail. A shell of very hot flames forms around a cooler core, and the temperature gradient decreases from the edge of the pan to its center. In the outer regions of the shell, the feedstock predominantly undergoes combustion, whereas cracking reactions increase towards the center. This temperature gradient leads to the formation of carbon black with very broad particle size distributions, which are a typical feature of lampblacks. The conical shape of the hood is required by the process.

The function of the ceramic material heated by the flames is to radiate the heat and vaporize the feedstock similar to a surface vaporizer. Easily vaporized oils lead to higher concentrations of hydrocarbons and thus to larger particle blacks. Since the feedstock has to be vaporized before it can react and since the vaporized portion of the oil is constantly replaced by fresh preheated oil, non-vaporizable, partly polymerized substances remain in the feedstock dish. These are drawn off from time to time and replaced by fresh oil.

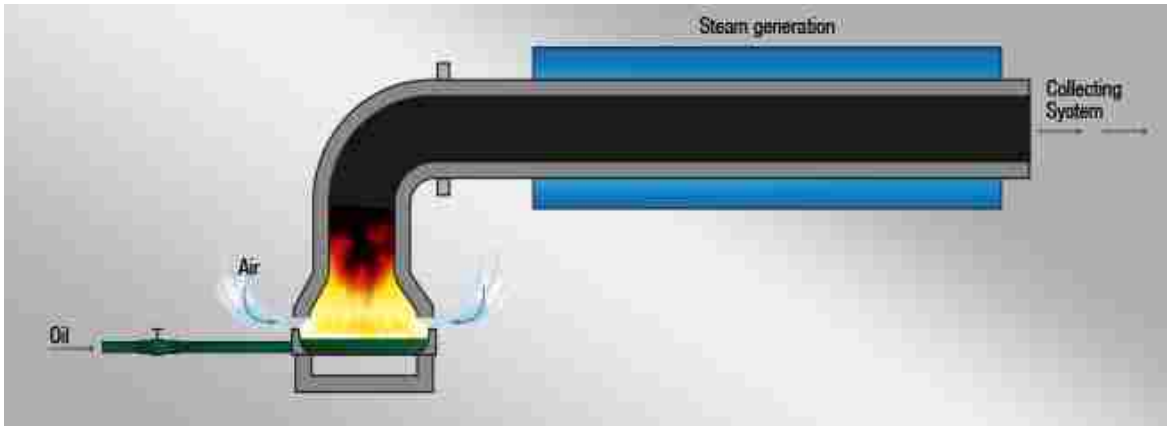

Figure 1.8. Lampblack process (J. B. Donnet, R. C. Bansal 1993)(https://pentacarbon.de/wiki/)

1.2.1.3. Channel black process. The channel black process is also known as the gas black process. In the past, the channel process for carbon black manufacturing played an important role, when it was on channel blacks that the reinforcing effect of carbon black in rubber was discovered in the 20th centuring. In the past, channel black processes were used mainly in tire treads, where they were far superior to lampblacks. In the 1950s, channel black processes were manufactured mostly in the United States. and exported worldwide, since their raw material to supply the industry, natural gas, was inexpensive there and available in enough quantities (Anonymous 2011; J. B. Donnet, R. C. Bansal 1993; Pundlik et al. 2013; Wójtowicz, Bassilakis, and Serio 2004).

This was not the case in Europe, which resulted in the investigation of different procedures, and in 1935 Degussa successfully developed the gas black process. The properties of these blacks were to the first blacks. They quickly gained a channel of gas black plants significant as reinforcing blacks, and a number in Europe constructed the process of the gas black is depending on the fundamentals of the decomposition of the thermal oxidative and the open system operation, where from the flames diffusion formed the carbon black. Free access for the air to the process resulted in oxidation of the surface, and consequently manufacturing acidic blacks (Anonymous 2011; J. B. Donnet, R. C. Bansal 1993). Thus the process of gas black utilized the oil in vaporized phase instead of natural gas, with coal tar which was distillated being the feedstock preferred. This feedstock (oil) is heated in the vaporizer, and the vapors that result are carried by a gas that is hydrogen-rich to the burners, the flames from which are allowed to hit on cooled water rollers. The carbon black mostly formed is deposited on these rollers, with the rest being collected as shown in Figure 1.9. Both carbon black streams are combined and processed

further.The pigment process is much more flexible than the lampblack process (Anonymous 2011; J. B. Donnet, R. C. Bansal 1993).

Although the access to air is free and is only controlled by diffusion, the process of charging the carrier gas with vaporized oil provides a means of achieving the desired primary particle size or specific surface area. Primary particle size ranges from 10 to 30 nm. Extremely fine particles can thus be obtained with the gas black process. It is not possible, however, to influence carbon black structure. Having lost their significance as reinforcing blacks, gas blacks are now mainly used as pigment blacks. It is an application for which they are particularly suited because of their acidic surface oxides. In many cases, this acidity is increased by oxidative after-treatment (Anonymous 2011; J. B. Donnet, R. C. Bansal 1993; Tomasini et al. 2012).

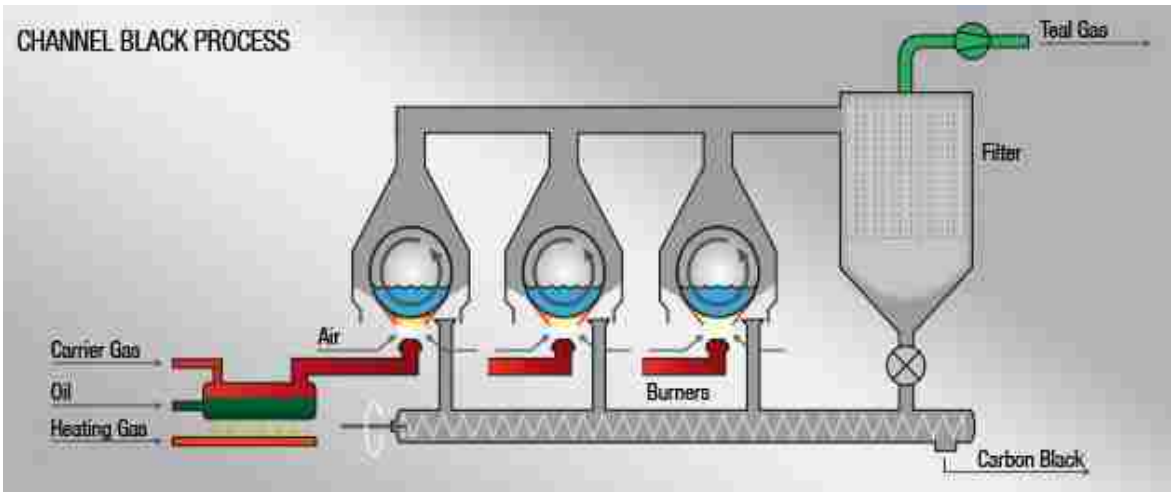

Figure 1.9. Channel black process or gas black process
(J. B. Donnet, R. C. Bansal 1993)(https://pentacarbon.de/wiki/)

1.2.1.4. Thermal black process. It is called “thermal black process”, due to the system that depends on the thermal decomposition in the absence of oxygen and operates in a closed system. One characteristic is that it is a cyclic process. The reactor in this process is shown, in a vertical view in Figure 1.10 and consists of a refractory lined furnace

that is fitted with a structural grid of fire bricks to increase the interior surface area. In the reactor in this process, heating up and decomposition cycles alternate each 5 to 8 min. Through the heating cycle, the temperature degree level will be reached when the fuel with air will burn in the reaction chamber. Then the air feed is stopped, the feedstock introduced, the waste gas vents closed, and the cycle of the decomposition begins. Inside the internal reactor. The feedstock will decompose to hydrogen and carbon black.

The carbon black then will separate from the gas stream, and subsequent processing will take place as described previously for furnace black. The most economical process configuration is when the reactors are coupled in tandem operation, as shown in Figure 1.10. This kind of processing has two reactors: the first reactor is on the heating cycle, and the second is in the decomposition cycle. When there is a gas feedstock, the hydrogen gas is produced in the second reactor and can be used to heat the first reactor. The first reactor starts the decomposition cycle, and the second reactor is reheated. Then for the first reactor, the temperature falls in the cycle and increases in the second reactor during the heat cycle. At the set point, the cycles are reversed.

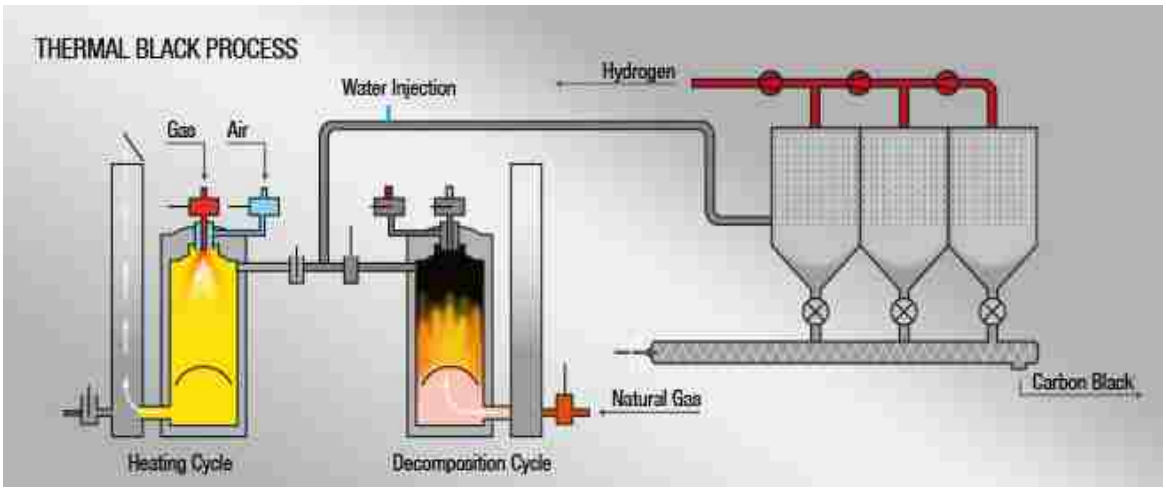

Figure 1.10. Thermal black process (J. B. Donnet, R. C. Bansal 1993)(https://pentacarbon.de/wiki/)

The hydrogen that is used in the heat cycle allows the gaseous hydrocarbon feedstock to be utilized to optimum since most of the hydrogen produced is burned to preheat the reactor, and most of the carbon is converted to carbon black. If oil is used as feedstock, the hydrogen produced is often too contaminated to be used in the heat cycle and is burned for other processes that are heat intensive. In order to differentiate, it is common practice to refer to the product from the two feedstock types as either gas thermal or oil thermal. These days the use of thermal black is limited to specialty applications in which their unique compounding properties cannot be matched with other fillers or filler combinations.

1.2.1.5. Acetylene black process. Acetylene black system, are manufactured in closed reactors by using the thermal decomposition method in the absence of oxygen. While the thermal black feedstocks could only be decomposed in an overall endothermal reaction, acetylene is thermally unstable and, after a start-up phase, can be split into hydrogen and carbon black in a highly exothermal reaction. The heat released has to be dissipated, which is achieved by the water-cooled cylindrical reactors. After the reactor has been heated briefly by burning acetylene, the air input is stopped, permitting the formation of carbon black. This reaction continues until the flow of feedstock is interrupted. Due to its reaction conditions and the unique feedstock properties, acetylene black differs from other carbon black grades.

The comparatively long residence time, the homogeneous hydrocarbon feedstock, and the considerable heat generated by the reaction yield very pure carbon blacks that exhibit a greater degree of crystallization than blacks obtained by the other methods previously mentioned. The shape of the primary particles is definitely not

spherical, and because aggregation of the particles is promoted by the high reactor feedstock concentrations, acetylene blacks are characterized by high structure. It is therefore difficult to densify acetylene blacks and impossible to pelletize them with these inherent physical limitations, and because of their electrical properties, acetylene blacks are used primarily as conductive blacks in electric cells and conductive and antistatic rubber and plastic applications.

1.2.2. Motivation. The thermal carbon black process depends on its operating conditions and design parameters. This study focused on the thermal black process due to the purest carbon forms and extremely low particle aggregation provided in this system.

This kind of process has easy and good mixing and dispersion, and even has smooth extrusion, excellent properties for processing and dynamics, and reduced energy costs due to improving the melt flow index of black plastic compounds.

1.3. RESEARCH OBJECTIVES

The overall objective of this work is to advance the understanding and the knowledge of the carbon black production with different conditions. Specifically, the goal of this work is to use the measurement techniques for sample characterization such as X-ray diffraction (XRD), scanning electron microscopy (SEM), Brunauer-Emmett-Teller (BET), Fourier-transform infrared spectroscopy (FTIR), and gas chromatography (GC). Determining the atomic and molecular structure of a crystal by XRD, producing an image result from interactions of the electron beam with atoms at various depths within the sample by SEM, analyzing surface area analysis by BET, and obtaining an infrared spectrum of absorption or emission of a solid, liquid or gas by

FTIR, and analytical chemistry for separating and analyzing compounds that can be vaporized without decomposition have been studied in this work. The completion of this work will enhance the understanding of the performance of high-temperature reactors with different feedstocks and conditions.

It also will provide data for benchmarking computational fluid dynamics (CFD) in a carbon black system with upset conditions.

The obtained knowledge of the effect of conditions on the manufacturing of the carbon black will facilitate the need for a detailed assessment for enhancement of the production level, as well as to advance the development of the reactor behavior, thus optimizing the production quality.

1.4. THESIS ORGANIZATION

A brief, general discussion of the carbon black production, manufacturing processes, physiochemical properties, and many other details, all are provided in section 1. Description of the experimental setup and work is in section 2. Characterization the powder and gas samples by using different measurements techniques in section 3. Section 4 provides the results and discussion. Finally, section 5 summarizes the study and provides the recommendations for future work.

2. EXPERIMENTAL WORK AND DESIGN

Extensive studies have been conducted on the thermal black carbon operational conditions on the production samples, such as surface area, particle shape and gas characterization, by using different measurement techniques. This study has enhanced our understanding of the reactor behavior and optimized the operating conditions in order to reach the purest carbon black production.

2.1. THE CARBON BLACK PRODUCTION PROCESS DESCRIPTION

As shown in Figure 2.1, the carbon black (CB) production process has been set up and located in *high temperature - High pressure Lab, Bertelsmeyer Hall, Chemical and biochemical Eng. Dep, Missouri University of science and technology.* This process consists of three main parts: first, the feedstock, second the main reactor, and the third is called quenching and output products. Examples of specific feedstocks include *Methane, Argon, Hydrogen, and Oxygen*. As shown in Figure 2.1, all feedstocks are connected to mass flow controllers (MFCs) and these valves are connected to the control box.

The main feedstock that will be used here is methane with a purity of 99.99%. On the other hand, Ar and H_2 gases will be used as diluent materials for different feedstock concentrations. As shown in Figure 2.1, the major parts of the CB system will include the following:

1. A bubbler tank will be used to saturate the feedstock with aromatic hydrocarbon.
2. Reactor tube assembly inside the resistive heater.
3. Unheated reactor section downstream of heater insulated with refractory.

4. Sliding sampling probe for length of the reactor.
5. Quench tie-in point.

The feedstock (methane gas) flowrate varies from *0.013-0.033 kg/hr*, and the diluent flowrate for Ar and H_2 will vary from *0-0.58 kg/hr* and *0-0.03 kg/hr*, respectively. The Ar will also be used as blanket gas to protect the graphite heater. Feedstock injector assembly is where the feedstock is mixed by the diluent gas, and blanket gas is introduced to protect the graphite heater.

The bubbler tanks is used for this project have a five-gallon stainless steel tank (1.5" diameter) and are used to get better resolution of the amount of aromatic hydrocarbon used to enrich the methane gas. The line coming from the MFCs is connected to the bubbler as a submerged tube inside the tank in order to make the methane flow as bubbles within the aromatic hydrocarbon. This bubbler tank is taped with a taped heater to heat up the aromatic hydrocarbon and conduct the temperature-aromatic flow calibration. Also, it is attached to a liquid level indicator to monitor the aromatic level.

The feed that comes from the bubbler will go into the reactor, where the length is about 19" before the heater. The feedstock is introduced into the reactor in addition to the oxygen gas. Also, the argon gas that was used as blanket gas to protect the heating element is also injected through the injection part. Inside the injection part, the reactor will be attached and insulated to avoid the heat loss. It will be insulated from the outside as well. The reactor assembly will be made of non-porous dense refractory material such as a graphite or high-purity alumina, which can hold temperature up to $2000^{O}C$. The thickness of the reactor will be minimum, about ½" is to ensure the mechanical integrity. The first part will be the reaction zone, where the reaction is carried out with the feedstock to produce CB.

Figure 2.1. Carbon Black Process

The heater will be made of graphite component (circular cross section with 4" diameter and 19.5" length) attached to two copper plates, where these three parts form the heating element. The heater will be shielded by a cooling system that is made of a non-conductive coated metal block where a cooling water flows inside it to maintain low outside temperature.

The power supply for the heater will be supplied from a voltage transformer where the primary line will be 480 V and 38-40 Am and the secondary line is 10V and 2312 Am. Three flow switches are attached to the cooling system for safety purposes, and it is designed to shut the power off on the heater when there is not enough cold water circulation. The temperature of the heater is maintained by temperature controller attached to c-type thermocouple. For this reason, a data acquisition system (DAQ) from National Instrument Inc. was used to monitor the temperature, and pressure and control the solenoid valves used to pulse nitrogen gas into the filter baghouse. The data acquisition (DAQ) model used was NI cDAQ-9184. Three different modules were installed in the DAQ, NI9213, NI9203, and NI9472. Two types of thermocouples were used to distribute along the process, K and C types.

The C type was installed in the heater to monitor the temperature of the heating element, the outside wall of the reactor in the heating zone, the outside of the reactor in the quench zone, and the temperature of the oxygen port at the injection part. The K type was used to measure the temperature of the bubbler, the water circulation inside and outside the heater, and on the filter assembly. Six pressure transducers were used in the system to monitor if there was any clogging inside the system. The thermocouples and pressure transducer locations in the system are shown in Figure 2.2.

Two type of reactors were used a graphite and alumina. The dimensions for the graphite reactor were 40” long and 3” ID with 0.5” thickness. For the alumina, 40” long with 3” ID and 0.25” thickness. The alumina reactor was used at the beginning for testing and eliminating the axial heat loss. It was replaced with graphite reactor as the process was running about 1500^{o} C, which is close to the max operating temperature of the alumina. The figure below shows the inside of the alumina reactor while running under 1500^{o} C. The graphite reactor was used instead as it can hold higher temperatures.

Figure 2.2. The DAQ system (Right) and the Thermocouples Distribution Along the Heater/ Reactor (Left)

The only challenge was the reactor thickness (0.5”), which could cause axial heat loss and eventually affect the product characteristics. To avoid the heat loss, two thermal barriers were installed. The thermal barrier material was a ceramic insulation (0.125” thickness) that could hold extremely high temperature. A step cut was made in the reactor to install two layers of the ceramic insulation on each side. A masking tape was used to hold the whole reactor together. The unheated part of the reactor was 5’in long and equipped with thermocouples to monitor the temperature variance through the reactor. The heat loss inside the unheated segment should be less than 100^{O}C due to the flow of the diluent gas. The quenching zone has a nitrogen gas injection port, nitrogen gas will quench

the reactor tail gases and reduce its temperature to about 650^{O}C. Temperature thermocouples are already installed at the quenching zone to maintain a specific temperature by injecting the nitrogen gas.

The reactor system will be operated under a high range of temperature. It will require carful procedure in order to achieve successful process output. The reactor's temperature will be measured by three temperature thermocouples attached to the data acquisition system. Also one thermocouple will be used as a measuring element for the temperature control used to energize the heater used to heat up the reactor.

Then the quench section, which is made of stainless steel, is installed downstream of the heater after the reaction zone. Nitrogen gas injected after the reactor to cool off the hot exhaust gas. The filter section consisted of two eyebolt cover filters connected in parallel by one two-way valve. Each filter had a sample container attached at the bottom to collect the carbon black sample, and it was equipped with perforated strainer basket. Filter bag of 1 micron was placed inside the filter house to separate the product from the gas. Sampling container was attached to the bottom of the filter house to collect the CB product sample. Two filters worked alternately. Filter1 worked and the filter2 was isolated. The samples were from the collected isolated one.

When cleaning the reactor, the reactor system will use oxygen gas for cleaning. The cleaning process will operate in a specific temperature that will be lower than ignition level. The product gases will send to the gas flare burner. The gas flare burner will be used to burn the product gases from the system, and a bouncing fire by propane will be used to maintain the flame inside the flare. For this purpose, as shown in Figure 2.1, a 55 gallon red barrel was used as an outside body for the flare system. The purpose of the system was

to burn the exhaust gases (the unreacted methane, the produced hydrogen, and any other combustible gases). A propane burner was installed inside the flare to keep a steady flame (bouncing burner). A liquid trap was installed before the flare system to prevent any flame to go back to the system. Two thermocouples (K-type) were installed on the flare's body and the hood system to check the temperature of the hot air flow to the ventilation system. In this work, the system will run with different diluent ratios between the methane and either hydrogen or argon gases. The system must be monitored all the time.

2.2. CHALLENGING DURING THE EXPERIMENTAL WORK

Several incidents occurred during operations, which means some adjustments in the process should be made for example, the C-type thermocouple that checked the temperature of the heating element and the one used to measure the temperature of the reactor had to be replaced every week due to the reaction that happened between the heating element and the thermocouple.

As the heating element is made of carbon and will react with the molybdenum material that the sheath is made of, so the hole made to let the thermocouple pass through had to become bigger.

Also, the thermocouple that monitored the temperature of the reactor had to be replaced, as it bent completely. This happened due to the countersink made to let the thermocouple sit in, and as the heat increased, and the thermal expansion of the graphite reactor bent the thermocouple. Instead of putting the thermocouple inside the countersink, it stayed on the surface to help it slide when the reactor expanded. The heater also was designed to reach almost 2000o C, but it was unable to because the resistance of the heating element was high.

The heating element was replaced with a new one that had less resistance so it could let more current go through and raise the temperature more. An external current meter was used to monitor the current flowing the heater. For safety precautions, three cameras were used to monitor the process while running. As shown in Figure 2.3, the reactor had been clogged after every several runs, as the carbon black accumulated inside the reactor, so it had to be opened every week for cleaning and inspection. The produced carbon black particle sometimes become very small (less than 1 micron) and cannot be separated by the filter and will pass through the flare. Some of the samples will stick inside the filter bag and cannot be removed from it.

Figure 2.3 Accumulation of the Carbon Black inside the Reactor

2.3. SAMPLE COLLECTION

This process has two types of samples that were produced. Solid and gas products. The solid product is the carbon black powder and usually will be separated from the gas by the filter section, where it will stick by the filter baghouse and drop in the sample container or stay on the bag itself. It will be removed from the bag and the bag should be cleaned for the next run, as shown in Figure 2.4. The gas sample, as shown in Figure 2.5, was collected from the gas sample valve at the downstream of the process after the filter section.

It will be removed from the bag and the bag should be cleaned for the next run, as shown in Figure 2.4. The gas sample, as shown in Figure 2.5, was collected from the gas sample valve at the downstream of the process after the filter section.

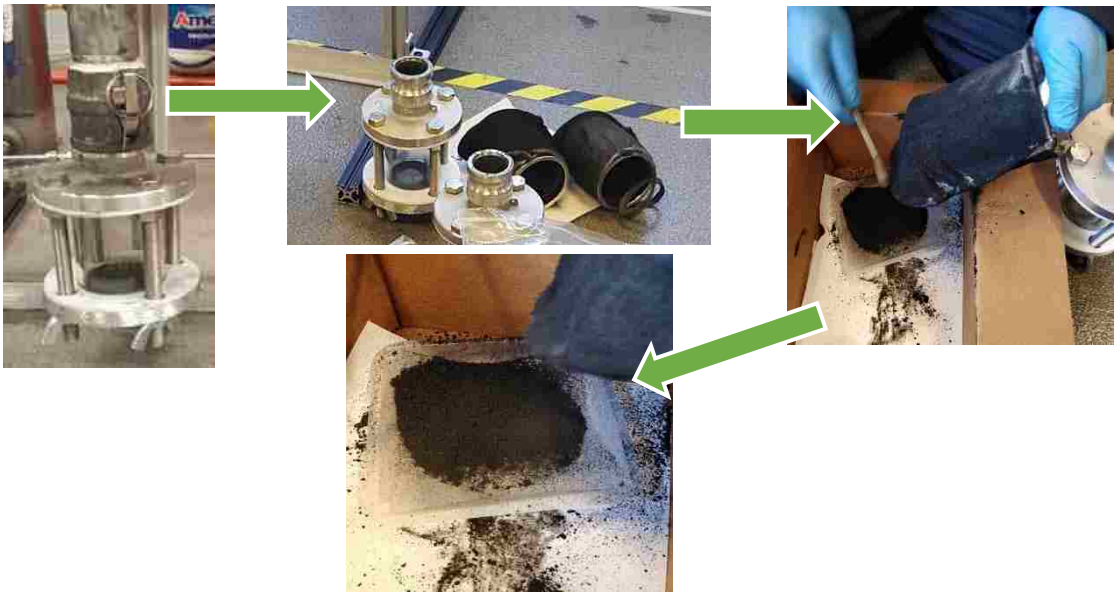

Figure 2.4. Carbon Black Powder Sample Collection

The sample was collected by a 2 liter gas sample bag and sent for analysis.

Figure 2.5. Gaseous Sample Collection

3. CB SAMPLES CHARACTERIZATIONS

The main part in this work analyzes the carbon black samples at different operating conditions. In this section, the characteristic measurement techniques SEM, BET, XRD, GC, and FTIR have been discussed in detail.

3.1. X-RAY DIFFRACTION (XRD)

X-ray diffraction is a non-invasive measurement technique that detects information about the structure of the crystal, chemical configuration, and the material properties. These kinds of techniques depend on detecting the intensity, where scattering of an *X-ray* beam hitting a sample is a function of scattered angle and incident beam, polarization, and wavelength or energy (Goldstein et al. 2003). X-ray diffraction studies proposed that carbon black was composed of small layers with the same atomic positions as graphite within the layers. The most important thing in this test is to identify a crystalline material and can provide information on unit cell dimension. The variable Lc represents the crystal structure thickness in c direction (Å), d_{002} represents distance between planes in c direction (Å). This parameters can be calculated from Scherrer and Bragg equation respectively (Jean-Baptiste Donnet, Bansal, and Meng-Jiao Wang 1993) (Goldstein et al. 2003). This measurement technique is used in the *AMCL* building in Missouri University of Science and Technology as shown in Figure 3.1.

Where: $Lc=1.84\ \lambda/\ \beta_{002}\cos\theta_{002}$

$d_{002}= \lambda/2\ \sin\theta_{002}$

θ= Bragg angle (degrees)

λ=wavelength (Å)

β= full width at half maximum intensity (FWHM) (radians).

Figure 3.1. X-ray Diffraction in the *AMCL*

Every analysis should have the following procedure for every sample:

a. Normalization to background measurement. As shown in Figure 3.2, to ensure consistency between analysis and samples, a background correction should be performed to normalize the diffractogram. This will ensure consistency of the FWHM measurement.

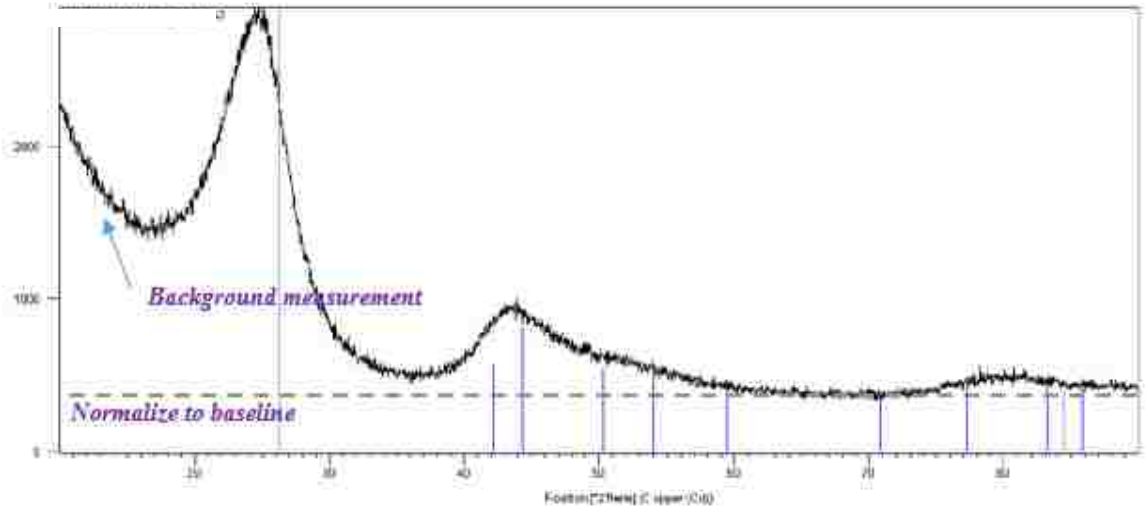

Figure 3.2. Normalization to background measurement

b. FWHM output from the XRD as shown in Figure 3.3, The XRD should be able to identify the Bragg angles at half maximum intensity and output the width in radians of the peak at that height. This width is important for utilizing the Scherrer equation and should be output for the (002) peak for every analysis. It is very important to do a background correction for every sample for consistency of the FWHM output as it is likely the measurement will be incorrect without.

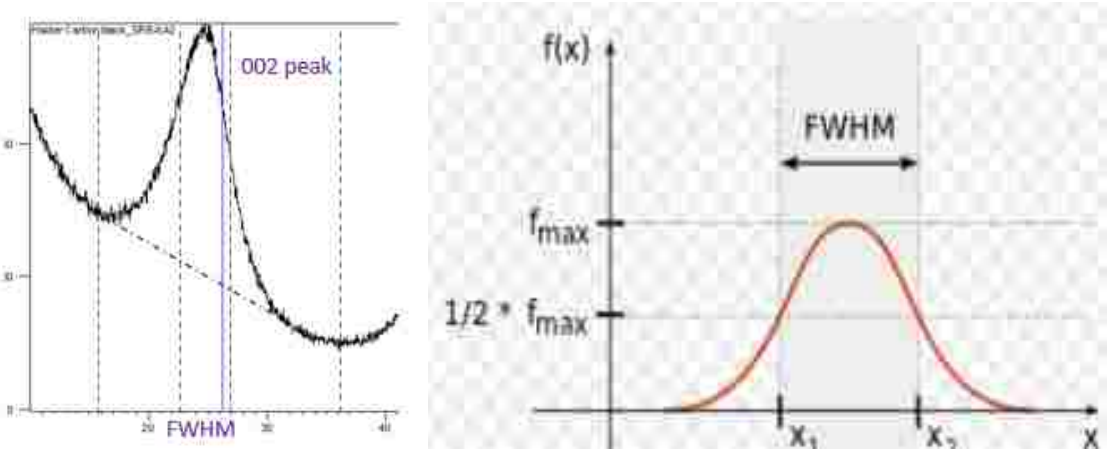

Figure 3.3. FWHM output from the XRD

c. Full span of the diffractogram saved and archived for reference. A diffractogram should be saved for every sample run following the determined naming convention for samples. Naming convention should be such that it can be easily tied to the same sample run on other analysis tools (BET, SEM, TEM, etc.). It is not necessary to run the full range of angles on the XRD but the range of the (002) peak should be captured (10deg – 40deg, 2theta) at the minimum. Excel / .csv output files should also be saved according to the naming convention on each diffractogram.

A summary Table 2 of all samples that have been run should include ID, FWHM, and Bragg angle at peak intensity, L_c, and d_{002} as shown below:

Table 2. Summary for results of XRD

Sample ID	FWHM	Bragg Angle @ peak	L_c	D_{002}
	Rad	Deg.	Å	Å

3.2. BRUNAUER, EMMETT AND TELLER (BET)

The BET (Brunauer, Emmett and Teller) method is commonly used for powder and materials research labs to measure the surface area by evaluating and quantifying the data of gas adsorption from the powder samples and expressed in units of area (m^2) per mass of sample (g), which is represented in (m^2/g).

The technique is referenced by several standard organizations such as ISO (International Organization for Standardization), USP (U.S. Pharmacopeial), and ASTM (An International Standards Organization).

At liquid nitrogen temperature and several partial pressures of nitrogen, the total and external surface areas were measured by evaluating the amount of nitrogen that adsorbed in the powder samples.

In this work, the Quantachrome Nova instrument has been used for this test (Brunauer, Emmett, and Teller 1938)(ASTM International 2012). This measurement technique was used in the McNutt Hall building in Missouri University of Science and Technology as shown in Figure 3.4.

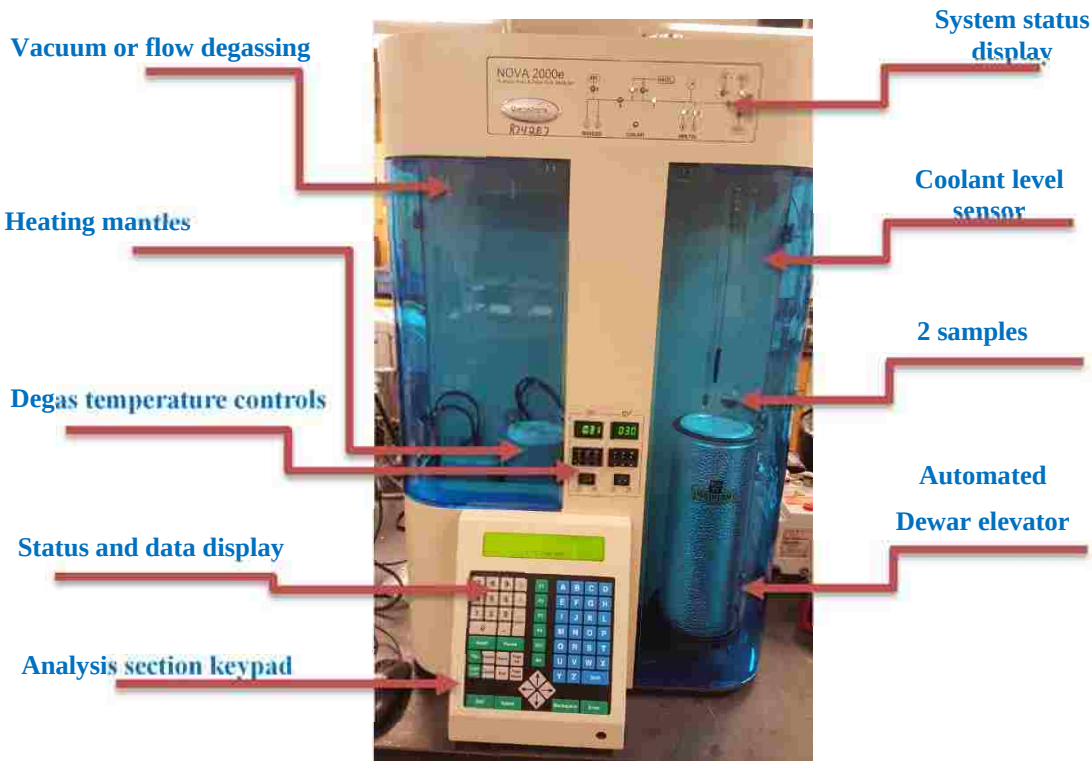

Figure 3.4. BET (Brunauer, Emmett and Teller)

The Langmuir theory is an extension of the theory for the molecular of the adsorption monolayer to the adsorption in multilayer with the following assumption: first, the molecules of the gas that adsorb physically as layers on solid surface infinitely; second, the molecules of the gas only adjacent interact with layers; and finally, the theory of the Langmuir is applied for each layer (Haiqing Liu 2016) (La Rosa et al. 2007).

The BET equation resulting is as follows:

$$\frac{1}{v[\left(\frac{p_0}{p}\right)-1]} = \frac{1}{v_m c} + \left(\frac{p}{p_0}\right) * \frac{c-1}{v_m c} \quad (1)$$

$$k = v[\left(\frac{p_0}{p}\right) - 1] \quad (2)$$

where p *and* p_0 are saturation pressure and equilibrium adsorbates at the temperature of adsorption, v is the quantity of the gas adsorbed, v_m is the quantity of the monolayer of the gas adsorbed, and c is the constant of the *BET*:

$$c = \exp\left(\frac{E_1 - E_L}{RT}\right) \tag{3}$$

Where E_1 *and* E_L are the adsorption heat in first layer and second layers, which is equivalent to the liquefaction heat, respectively.

The isotherm adsorption in Eq (1) could be plotted as a straight line way with the y-axis 1/k and the x-axis $\tau = p/p_0$ according to the experimental results. This is named the plot *BET* as shown in Figure 3.5.

The relation is linear in the equation and only continued in range $0.05 < p/p_0 < 0.35$. Slope is A, and I is the intercept for the line. Both are utilized to measure gas adsorbent quantity in the monolayer v_m, and the constant of the BET is c. The equations that follow could be used for calculation:

$$v_m = \frac{1}{A + I}$$

$$c = 1 + \frac{A}{I}$$

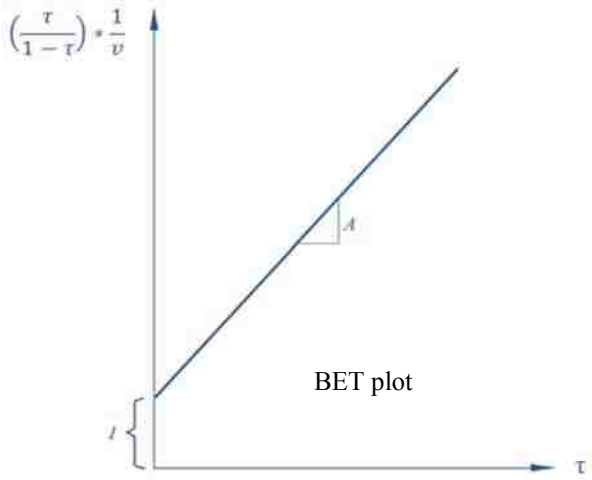

Figure 3.5 BET plot

The method of the *BET* is commonly utilized in science of the surface in the measuring of surface areas for powders (solids) in physical adsorption of gas molecules. The S_{total} is

total surface area and S_{BET} is the surface area for the sample (Bernal et al. 2011) are given by:

$$S_{total} = \frac{(v_m N_s)}{V} \quad (4)$$

$$S_{BET} = \frac{(S_{total})}{a} \quad (5)$$

where v_m in volume units is also the monolayer volume units of the gas adsorbate, N is Avogadro's number, s is cross adsorption section of the species adsorbing, V is the molar volume of the gas adsorbate, and a is the solid mass sample or adsorbent (Jianfeng ZHANG, Rong TU 2013). This test consists of two steps: vacuum degassing and gas adsorption analyzer.

3.2.1. Vacuum Degassing. This step is very important to dry the sample from any moisture it could contain and attain an accurate surface area. First, start with collecting samples from the container used for this reason.

Then, record the weight of the sample, and take a 0.1-0.5gm from the collected sample in order to use it in this test. Second, prepare a clean sample cell (bulb) and record the weight of the bulb when it is empty three times and take the average for precise weight.

Third, insert the sample (which is the powder) inside the cell (bulb) by using a delivery tube. Fourth, connect the cell (bulb) to the degassing part in the instrument and set the heater at the temperature 200ºC and covered this cell by using specific heating mantle around the cell and then turn on the heater. At this point, the vacuumed degassing will start with helium gas for 1hr as shown in Figure 3.6.

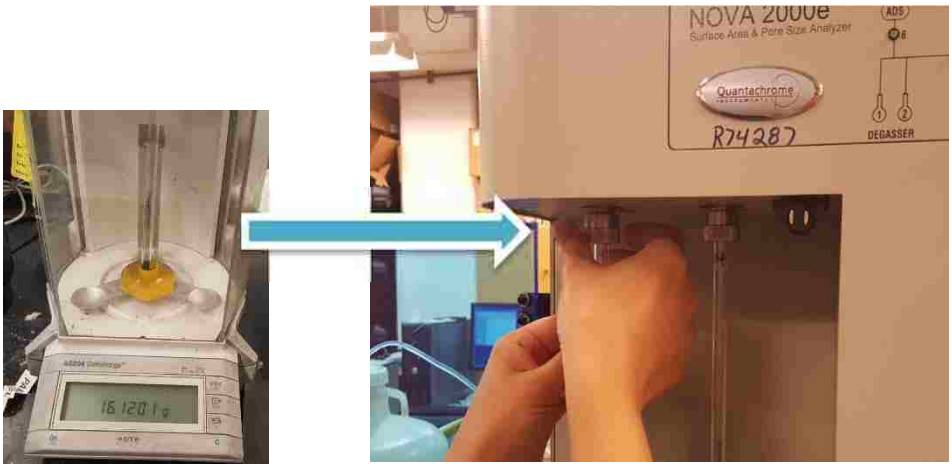

Figure 3.6. Connect the sample (bulb) to the degassing section after scale the powder

Then, set the heater at the temperature 200^{o}C and cover this cell by using a specific heating mantle around the cell and then turn on the heater. At this point, the vacuumed degassing will start with helium gas for 1 hr. Afterwards shut off the heater and release the mantle from the cell and leave the sample to cool down for 1 hr, as shown in Figure 3.7.

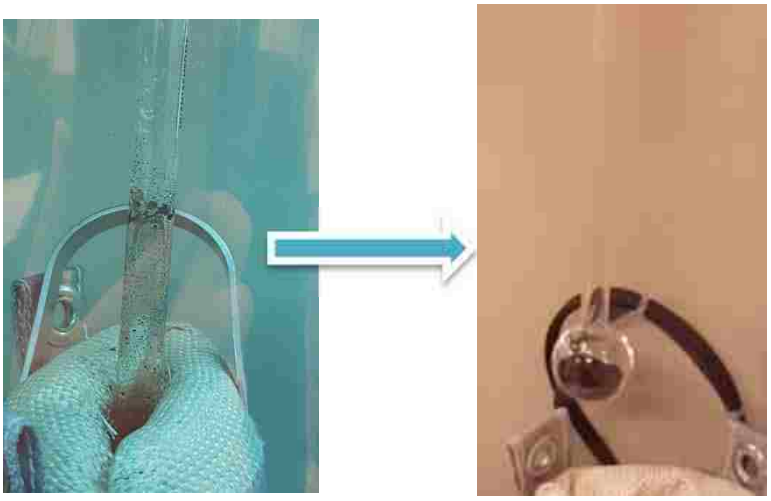

Figure 3.7. Heat up the sample to 200C and then remove the heating mantle to cool the sample

3.2.2. Gas Adsorption Analyzer. In this step, nitrogen gas adsorbed in the CB sample is at different saturated pressures to calculate the surface area which is following the multipoint procedure. This measurement took 11 points in each run to get accurate and correct surface area. After the degassing, record the weight for the cell with the dry sample three times and take the average: Mass dry sample = mass the cell with the sample - mass the empty cell

After that, connect the sample cell to the analyzer part in the instrument, and fill the Dewar (*1L* size) with liquid nitrogen and put the Dewer in the analyzer side, which is near to the sample cell. At this point, write the name of the sample and the weight in the software (NOVA version 11.02) for this device and start the analysis. This operation will take place for 1.5 – 2.0 hr. The highest surface area was 40 m^2/gm and the lowest one was 10 m^2/gm. These steps are shown in Figure 3.8.

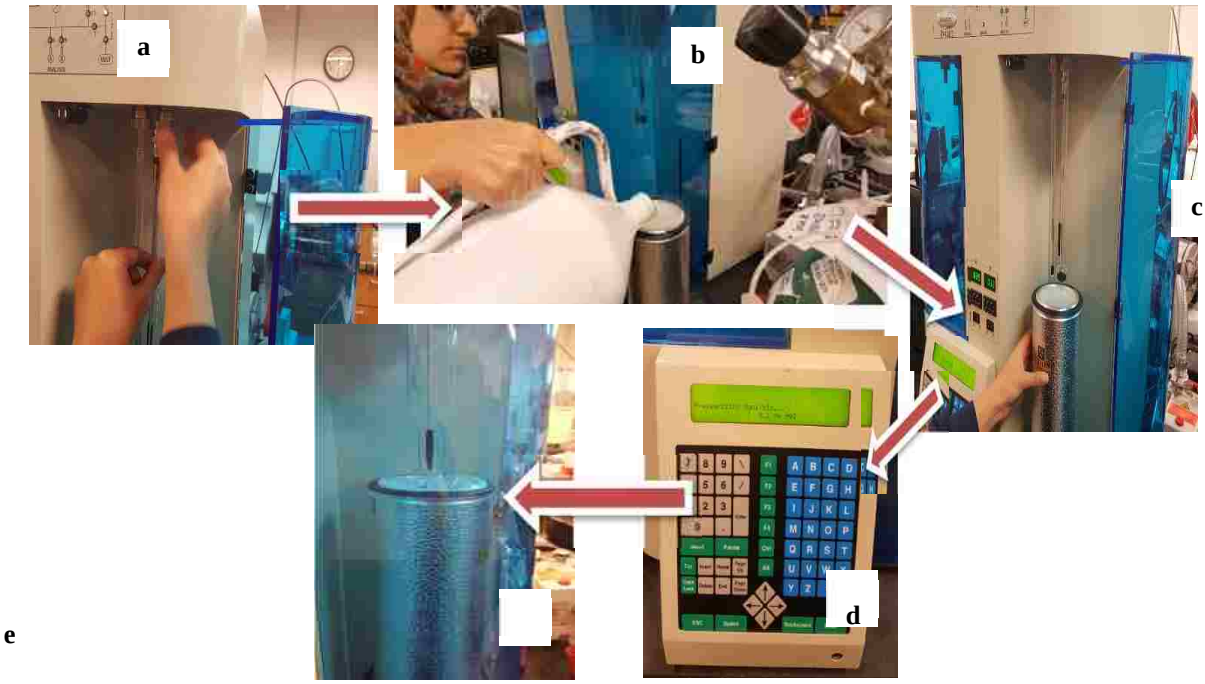

Figure 3.8. BET Test (a) Connect the sample to the analyzer section, (b) Full the Dewar with liquid Nitrogen, (c) put the Dewar at the analyzer section, (d) set the point and (e) leave the sample for 2hr

3.3. SCANNING ELECTRON MICROSCOPE (SEM)

Scanning electron microscope (SEM) is a kind of electron microscope which gives an image of a sample by scanning the surface of the sample with the beam focused on electrons. The interaction of the electrons with the atoms in the sample produce various signals that contain information about the topography and composition of the sample's surfaces. The beam of the electron is scanned in a raster scan pattern, and the position of the beam is combined with the signal detected to produce an image (J-B Donnet 1993);(Goldstein et al. 2003). Some of the samples selected for scanning have, higher surface area at many magnifications to see how the particles look and the aggregate shape. Before the SEM measurement, we have to prepare the samples, as shown in Figure 3.9. This the magnification test is followed for each sample: 4000X overview, 7000X overview, Focus on cluster at 15000x, Focus on cluster at more 30000X and Highest magnification 60000X. Our scan pictures showed that the particles had almost spherical shape and there were aggregate regions.

Figure 3.9. Carbon Black powder that prepared for SEM measurement.

3.4. GAS CHROMATOGRAPHY (GC)

For analytical chemistry in terms of gas characterization, the gas chromatography (GC) is a very useful for analyzing and separating compounds that could be vaporized without decomposition. Particular uses for GC include testing the purity of the substance or separating the different components of a mixture (the comparative amounts of such composition could also be specified). In particular situations, GC may assist and help in the compound identification. In chromatography preparation, GC could be utilized to prepare pure compounds from a mixture. As shown in Figure 3.10, the GC instrument consists of the following:

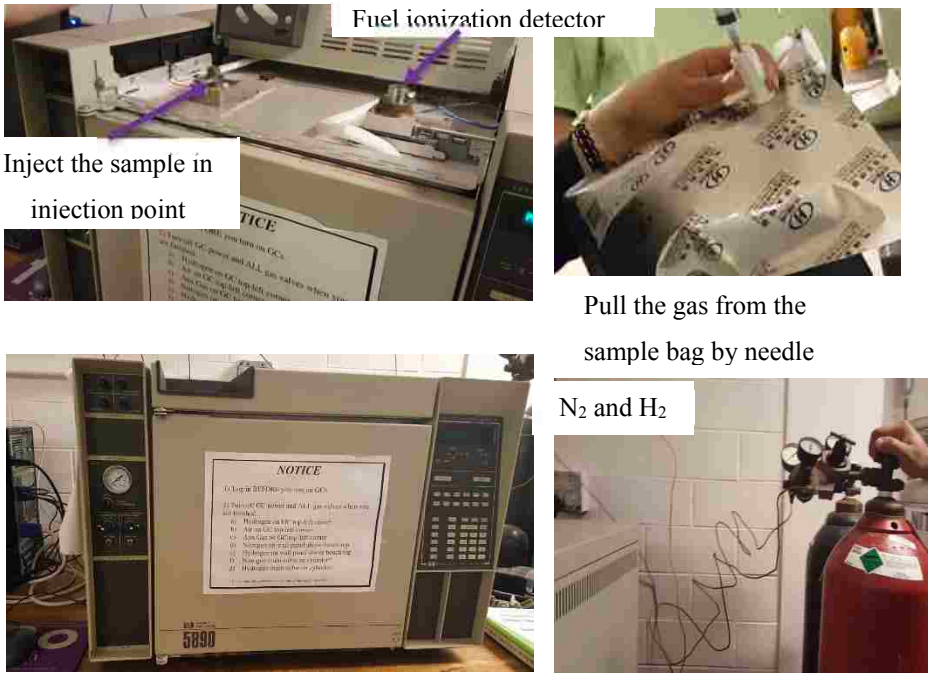

Figure 3.10. Gas Chromatography GC which placed in Chemistry department

The carrier gas is N2 (auxiliary gas), H2 gas (fuel ionization detector), injector temp 30C, the oven temp 30C and the detector temp 200C, column length was 30 m and using (S&T GC program) to acquire the results data. Steps of analysis:

1. Open the gases valves from the cylinders
2. Open the GC instrument.
3. Set the oven, injector and detector temperatures.
4. Open the program on computer and type the samples name and all information.
5. When the detector temperature reaches 200^{o}C, open the H2 gas, air, and auxiliary gas valves on GC instrument, then push the igniter bottom. The voltage detector should read from 20-50. If not, change the flow rate for the gases and push the igniter bottom again.
6. Use syringe with 5 ml to inject the gas sample inside the column and put septum rubber on the injector place.
7. Inject (1 ml) for all the samples and reference gases (CH4, C2H4).
8. From the results peaks on the GC program, we notice one peak after 4 min for all samples tested for 10 min (retention time). This peak is either CH4 or C2H4.

*The results from the GC looks not accurate because we are expected more than one peak so we are using the FTIR instead of the GC.

3.5. FOURIER-TRANSFORM INFRARED (FTIR)

Fourier-transform infrared (FTIR) spectroscopy is a technique utilized to evaluate and measure the absorption of spectrum infrared or the emission of a liquid, solid, or gas. The spectrometer of FTIR simultaneously over a wide spectral range will collect high-spectral-resolution data. This confirms a significant advantage over a dispersive spectrometer, which measures intensity over a narrow range of wavelengths at a time (Griffiths and De Haseth 2007)(Mattson 1978). In our work, NEXUS (470-FTIR) has been used for gas analysis with 4 cm-1 resolution and 16 scans and the gas cell dimension (25 cm length, 5 cm Diameter), as shown in Figure 3.11.

In our work, *NEXUS (470-FTIR)* has been used for gas analysis with 4 cm^{-1} resolution and 16 scans and the gas cell dimension (25 cm length, 5 cm Diameter), as shown in Figure 3.11. The reference gases analyze it first (methane, ethylene, acetylene, and ethane) with different compositions and compare it with the NIST (National Institute of Standards and Technology) spectra data as a reference spectra to ensure that our FTIR results match or are close to the reality. First of all, start with purging the gas cell (Figure 3.11) by using pure N_2 for 5-7 min to clean it from any H-C that could be inside the cell. This step is very important to get accurate and precise results.

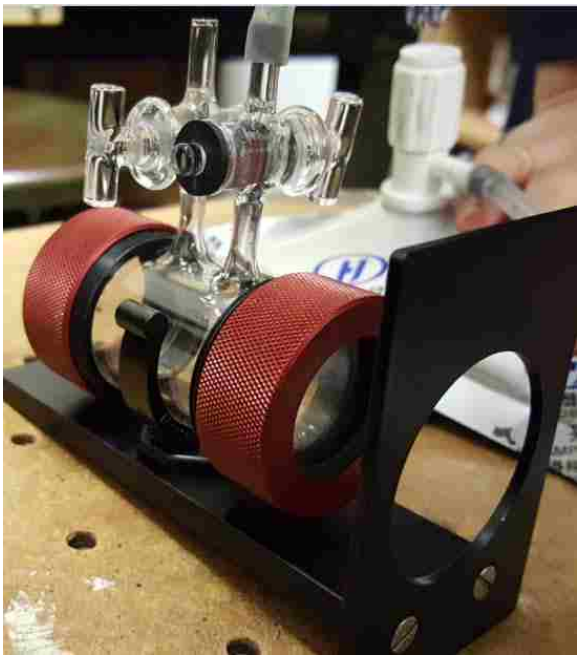

Figure 3.11. Gas Cell

Ensure that the lenses for the gas cell are clean and the caps are fixed probably because this might affect the beam direction. Then, set the dry air level to 40, and put the cell inside the FTIR, and collect the BKG (background) spectra. After that, fill the cell with

the sample (Figure 3.13) and return it to the FTIR, and then collect the spectra data from the computer for the sample.

Figure 3.12. Purging the gas cell by using N2

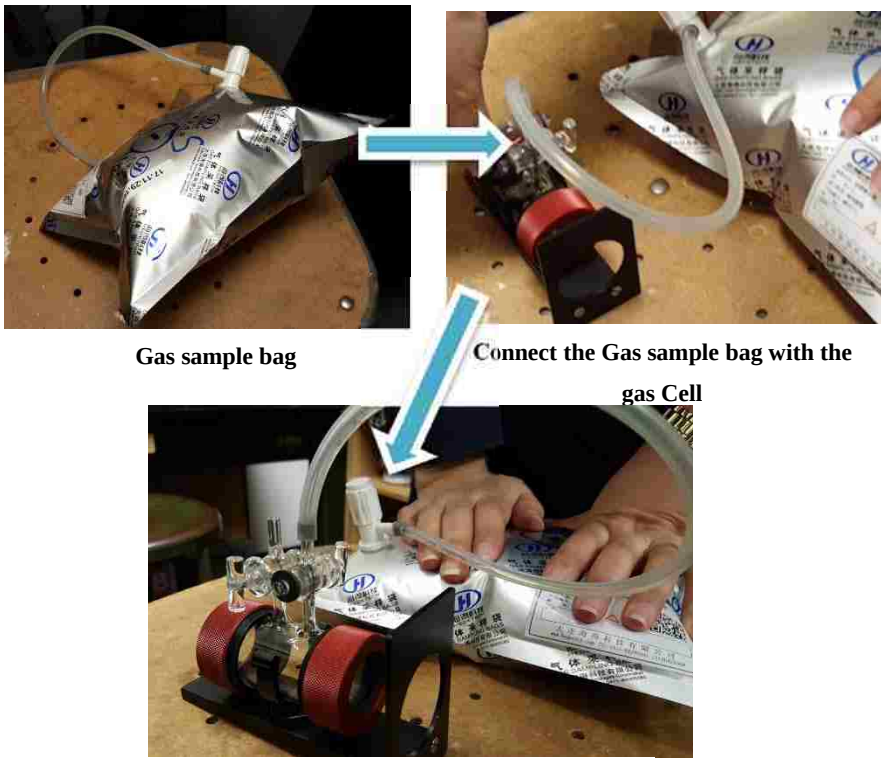

Figure 3.13. Steps of the gas cell filling

Connect the gas cell inside the FTIR device as shown in Figure 3.14 in order to analyze the gas sample. Two sample 2L bags were used in the test, to replicate the spectra test twice to obtain good spectra results. Complete flashing for the cell with pure N_2 in 5-7 min between each sample in order to clean it from any H-C that could be still inside the cell from the previous sample.

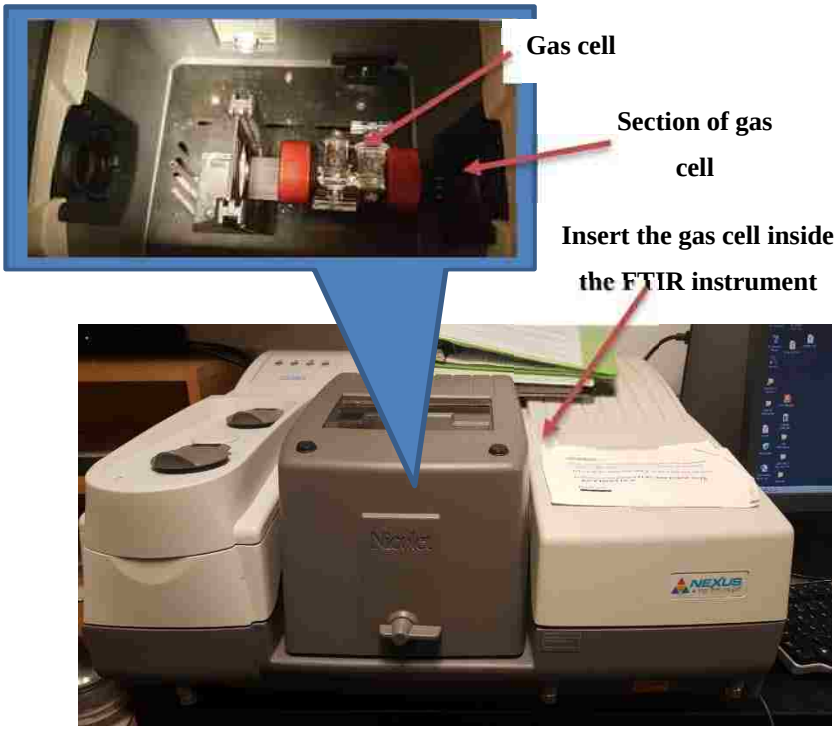

Figure 3.14. FTIR instrument placed in Chemistry department

4. POWDER OF CARBON BLACK AND GASSES RESULTS

4.1. BET RESULTS

More than 60 samples have been tested it in this measurement. This operation took place for 4 hr. below is a copy of the report of the BET analysis. The highest surface area was 40 m^2/gm and the lowest was 10 m^2/gm. Samples of BET results have been observed in Figure 4.1:

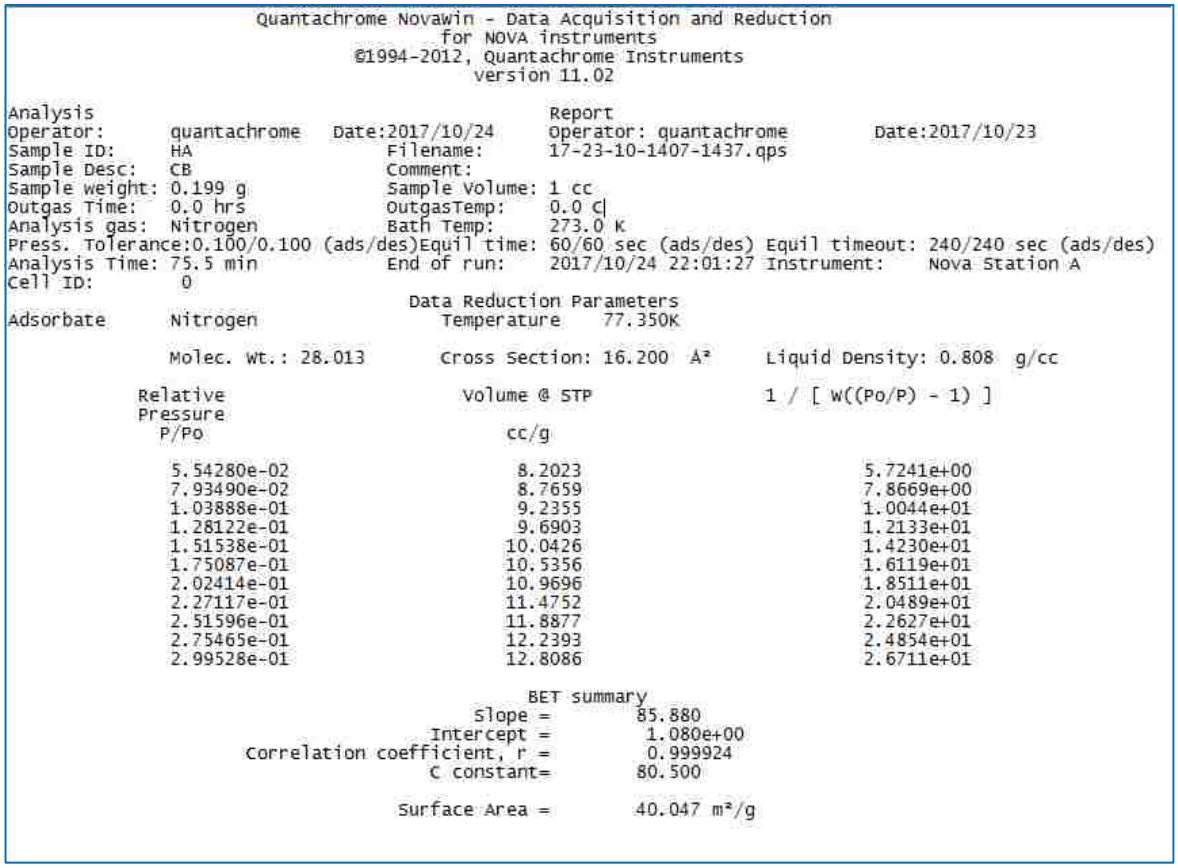

Quantachrome Novawin - Data Acquisition and Reduction
for NOVA instruments
©1994-2012, Quantachrome Instruments
version 11.02

Analysis			Report		
Operator:	quantachrome	Date:2017/10/24	Operator: quantachrome		Date:2017/10/23
Sample ID:	HA	Filename:	17-23-10-1407-1437.qps		
Sample Desc:	CB	Comment:			
Sample weight:	0.199 g	Sample Volume:	1 cc		
Outgas Time:	0.0 hrs	OutgasTemp:	0.0 C		
Analysis gas:	Nitrogen	Bath Temp:	273.0 K		
Press. Tolerance:	0.100/0.100 (ads/des)	Equil time:	60/60 sec (ads/des)	Equil timeout:	240/240 sec (ads/des)
Analysis Time:	75.5 min	End of run:	2017/10/24 22:01:27	Instrument:	Nova Station A
Cell ID:	0				

Data Reduction Parameters

Adsorbate	Nitrogen	Temperature	77.350K		
	Molec. Wt.: 28.013	Cross Section:	16.200 Å²	Liquid Density:	0.808 g/cc

Relative Pressure P/Po	Volume @ STP cc/g	1 / [W((Po/P) - 1)]
5.54280e-02	8.2023	5.7241e+00
7.93490e-02	8.7659	7.8669e+00
1.03888e-01	9.2355	1.0044e+01
1.28122e-01	9.6903	1.2133e+01
1.51538e-01	10.0426	1.4230e+01
1.75087e-01	10.5356	1.6119e+01
2.02414e-01	10.9696	1.8511e+01
2.27117e-01	11.4752	2.0489e+01
2.51596e-01	11.8877	2.2627e+01
2.75465e-01	12.2393	2.4854e+01
2.99528e-01	12.8086	2.6711e+01

BET summary

Slope =	85.880
Intercept =	1.080e+00
Correlation coefficient, r =	0.999924
C constant=	80.500
Surface Area =	40.047 m²/g

Figure 4.1. BET results report for one sample

4.2. XRD RESULTS

Figure 4.2 and 4.3 show one XRD result and other statistical data for one sample, respectively, after doing the normalization and calculation for the figure by using OriginPro

2017 software. These figures show that most of the samples are graphite. The results for FWHM, Bragg Angle Peak, Lc and D_{002} are shown in Table 3.

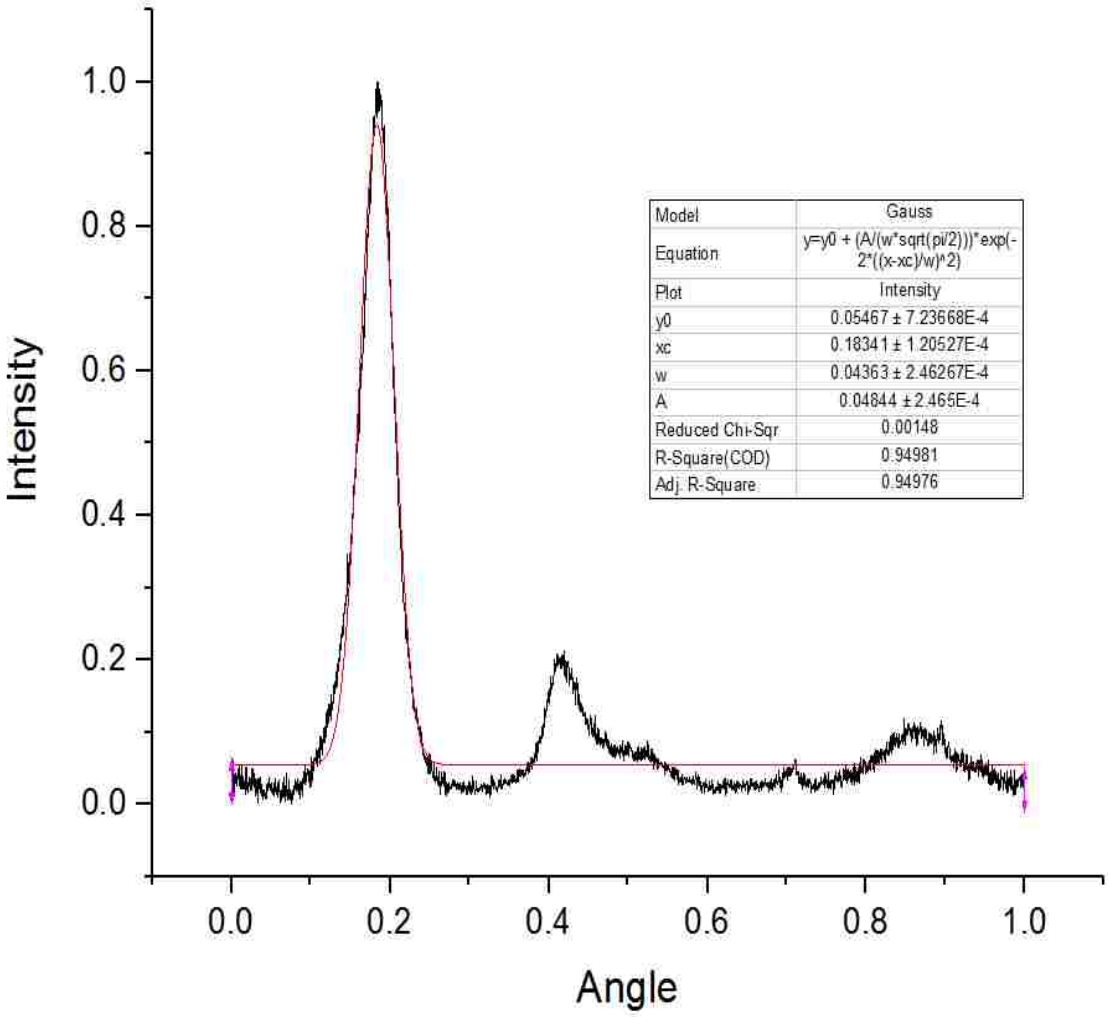

Figure 4.2. XRD analysis

Table 3. XRD analysis

FWHM	**Bragg Angle @ peak**	**Lc**	**D_{002}**
FWHM	**Bragg Angle@ peak**	**L_c**	**D_{002}**
Rad	**Deg.**	**A**	**A**
0.03176	12.75	91.50113	3.4899477

Nonlinear Curve Fit (Gauss) (12/20/2017 21:49:22)

Notes

Input Data

Parameters

		Value	Standard Error	t-Value	Prob>|t|	Dependency
Normalized1	y0	0.05933	--	--	--	--
	xc	24.875	--	--	--	--
	w	2.52281	--	--	--	--
	A	3.49909	--	--	--	--
	sigma	1.2614	0			
	FWHM	2.97038	0			
	Height	1.10665	0			

Reduced Chi-sqr = 0
Iterations Performed = 0
Total Iterations in Session = 0
Fit did not converge - reason unknown.
Some parameter values were fixed.
Standard Error was scaled with square root of reduced Chi-Sqr.
sigma, FWHM, Height are derived parameter(s).

Statistics

	Normalized1
Number of Points	3198
Degrees of Freedom	3198
Reduced Chi-Sqr	0
Residual Sum of Squares	0
R-Square(COD)	0
Adj. R-Square	3.12695E-4
Fit Status	Failed(-207)

Fit Status Code :
-207 : Fit did not converge - reason unknown.

Summary

	y0		xc		w		A		sigma	FWHM	Height	Statistics	
	Value	Standard Error	Value	Standard Error	Value	Standard Error	Value	Standard Error	Value			Reduced Chi-Sqr	Adj. R-Square
Normalized1	0.05933	--	24.875	--	2.52281	--	3.49909	--	1.2614	2.97038	1.10665	0	3.12695E-4

ANOVA

		DF	Sum of Squares	Mean Square	F Value	Prob>F
Normalized1	Regression	0	128.21114	--	--	1
	Residual	3198	0	0		
	Uncorrected Total	3198	128.21114			
	Corrected Total	3197	94.22448			

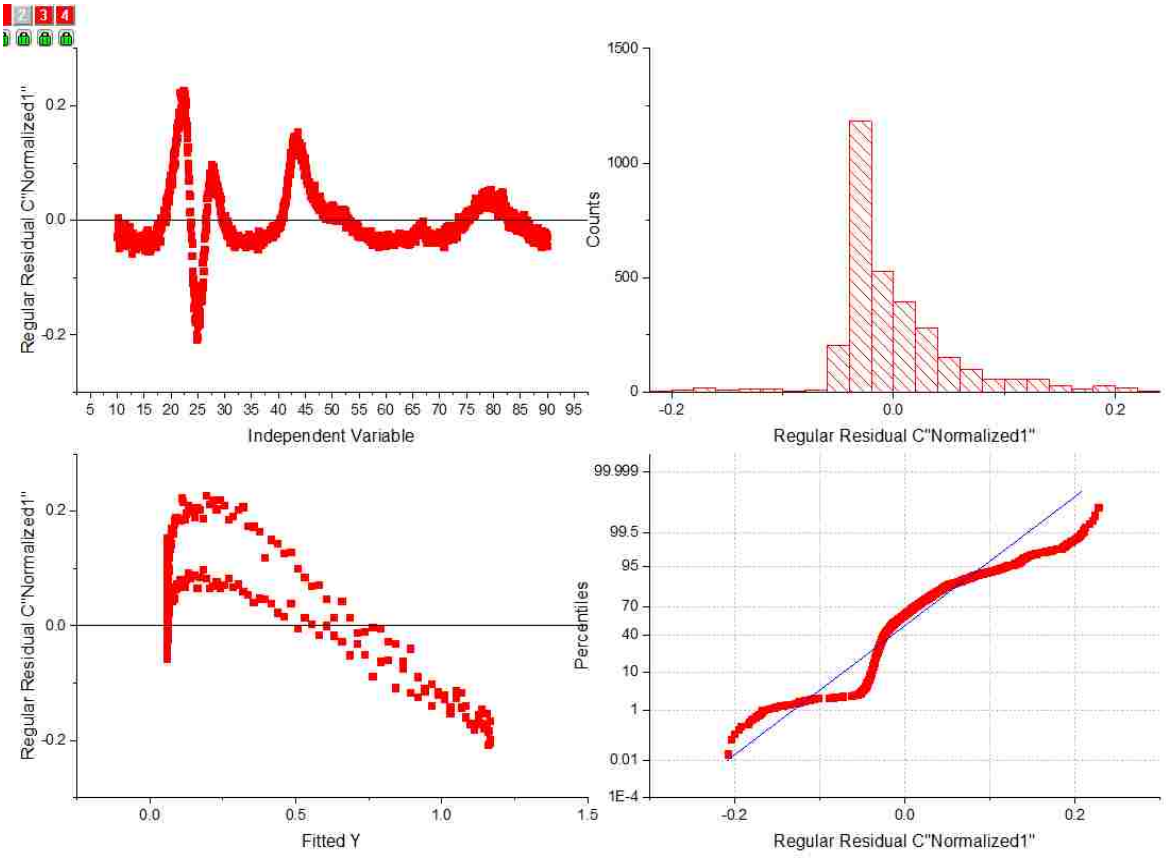

Figure 4.3. Other statistical data for XRD results

4.3 SEM RESULTS

As shown in Figure 4.4, the results, which were scanned by SEM, show the particles almost spherical shape and aggregate regions. These scanned pictures for the sample had the highest surface area at different resolutions. The SEM image for the sample with 40 m^2/gm is the highest one.

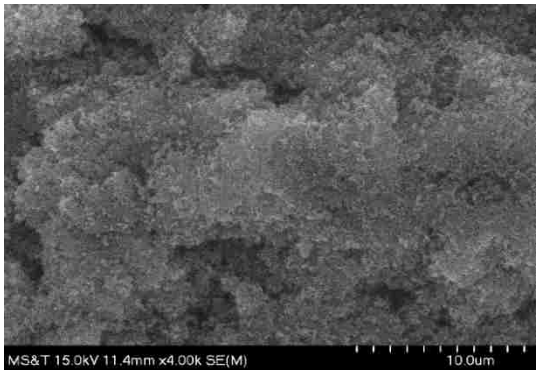

4000X magnification

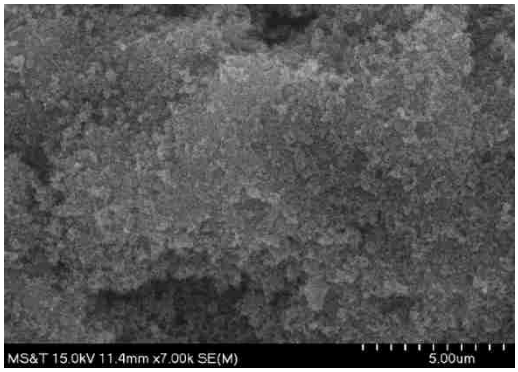

7000X magnification

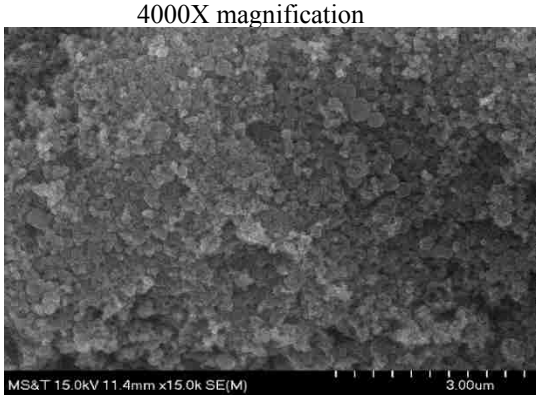

15000X magnification

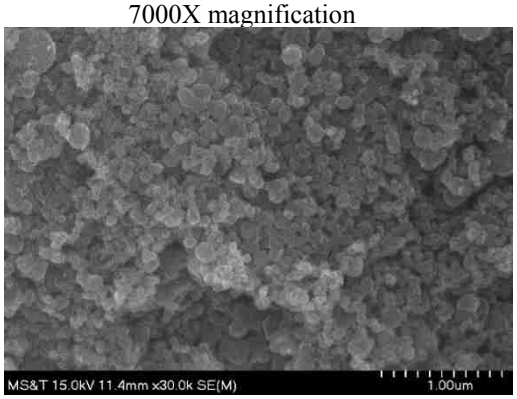

30000 X magnification

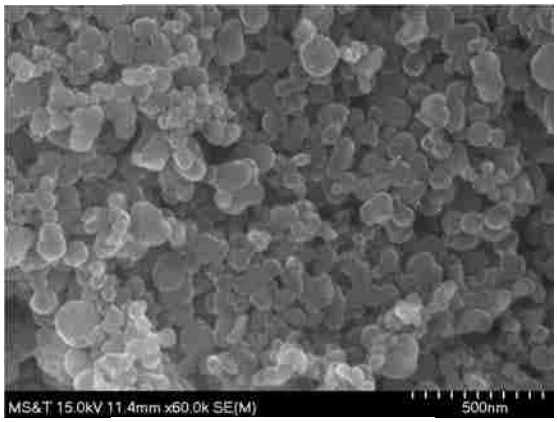

60000 X magnification

Figure 4.4. SEM images for carbon black sample at different resolution

4.4. GAS CHROMATOGRAPHY (GC) RESULTS

More than 16 samples have been testing it to find the gas analysis. At the beginning the references gases results have been shown in Figure 4.5 for methane and ethylene gases. Next the analysis taken place for real samples as shown in Figure 4.6.

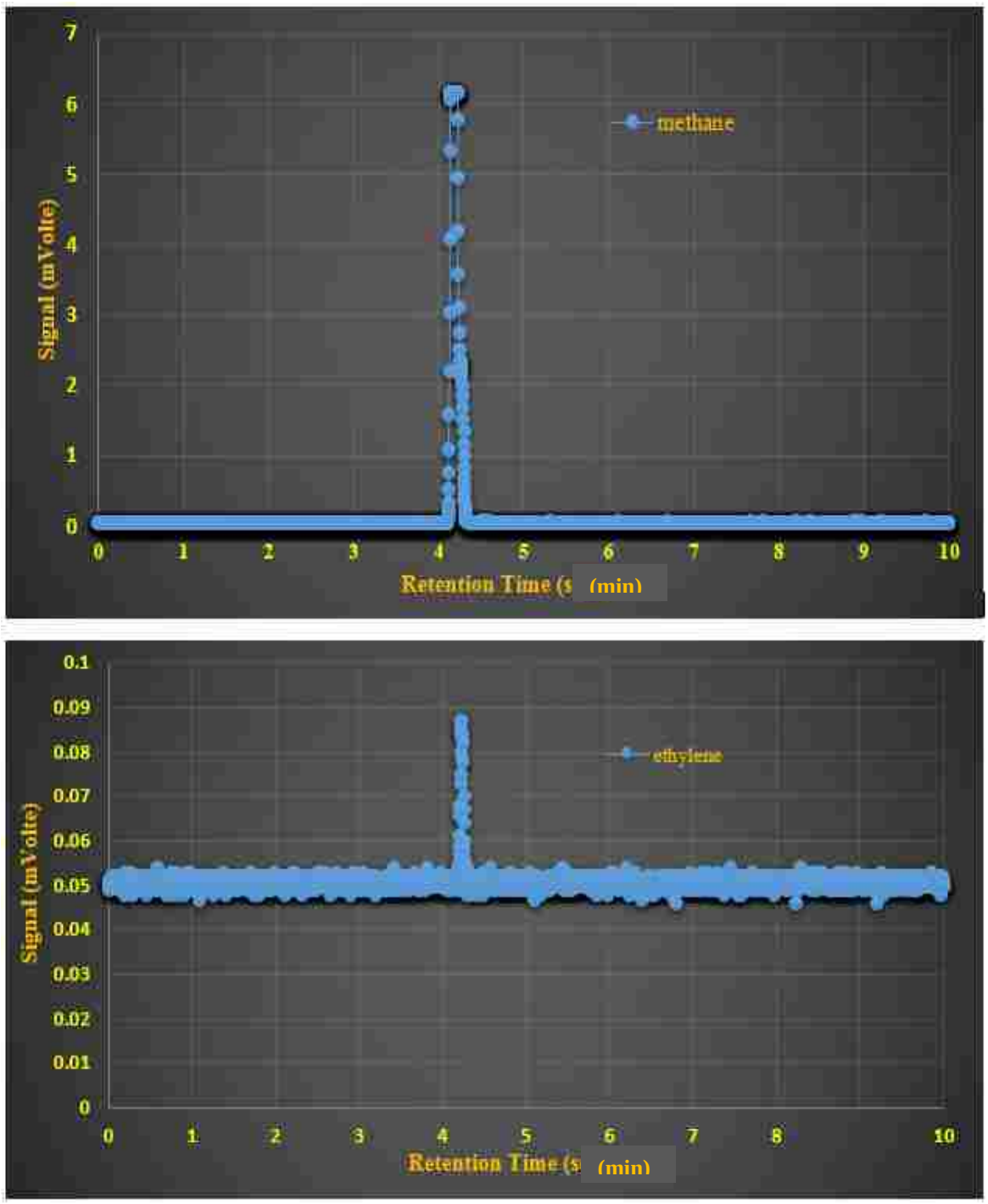

Figure 4.5. GC analysis for standard as references gases

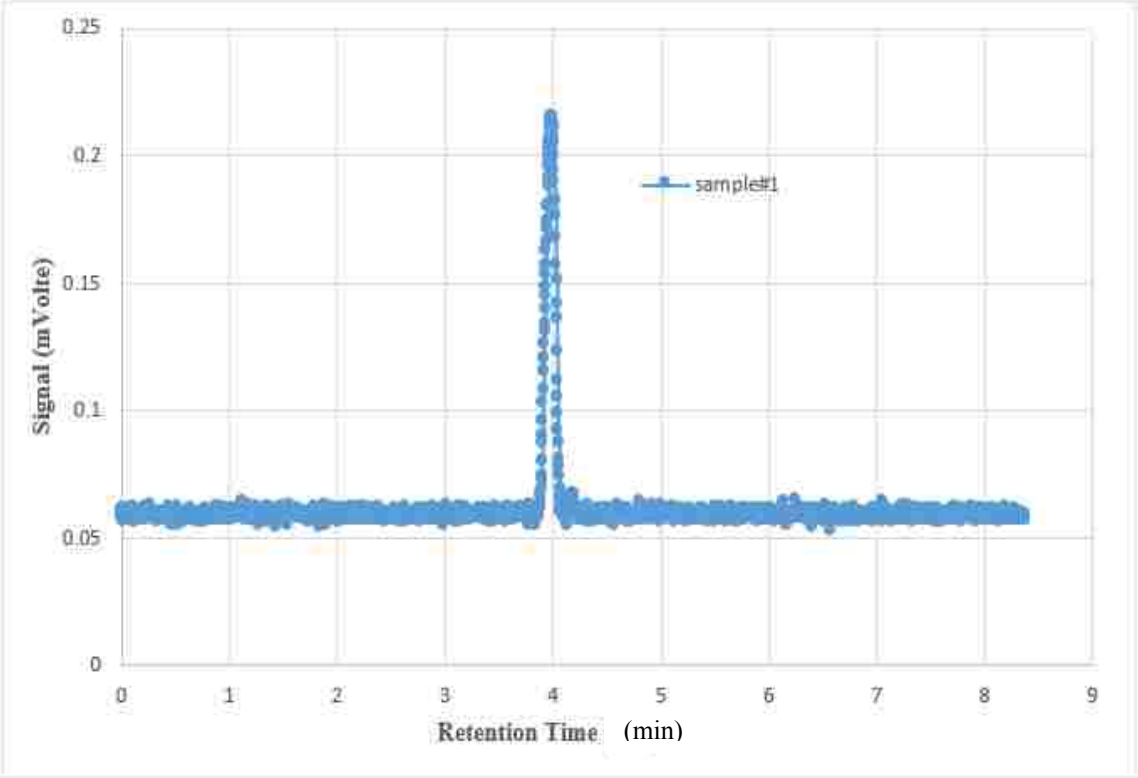

Figure 4.6. GC analysis for sample#1

4.5. FTIR ANALYSIS

The analysis started with the reference gases spectra, detection limitation, qualitative and quantitative analysis of the gases and finally sample of the results.

4.5.1. Reference Gases Spectra and Samples. We run the reference gases (methane, ethylene, acetylene, and ethane) with different compositions and compared it with the NIST (National Institute of Standards and Technology) spectra data as a reference to ensure that our FTIR results are matched or were close to the reality, as shown in Figures 4.7, 4.8, 4.9, 4.10, 4.11, 4.12, 4.13, 4.14, 4.15, 4.16 and 4.17. Two sample spectra are shown in Figure 4.18 and 4.19.

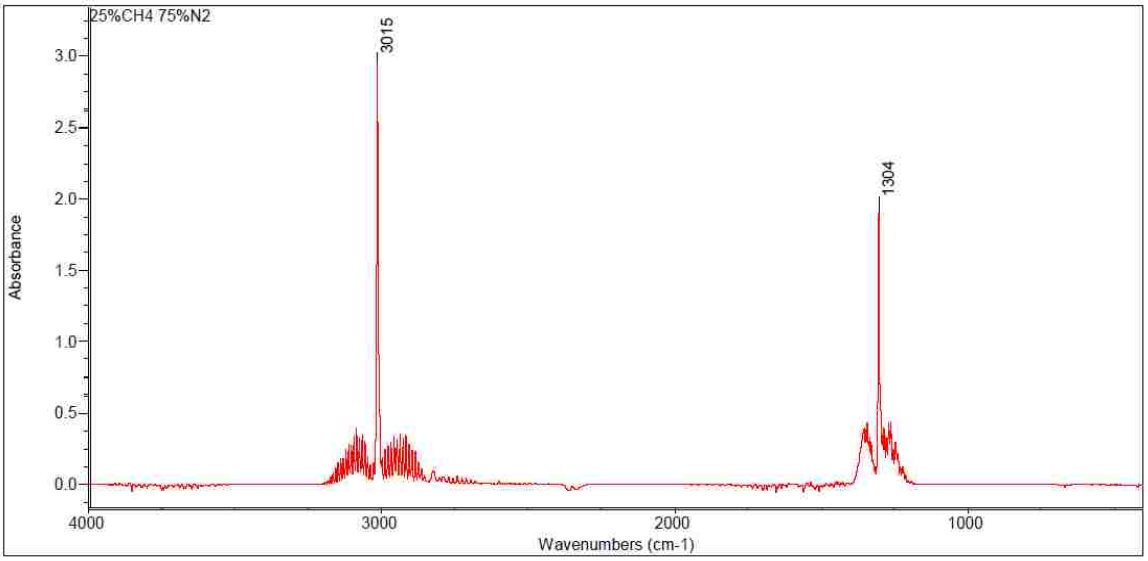

Fri Oct 13 15:42:46 2017
FIND PEAKS:
Spectrum: 25%CH4 75%N2
Region: 4000 400
Absolute threshold: 1.267
Sensitivity: 50
Peak list:

Position:	3015	Intensity:	3.020
Position:	1304	Intensity:	2.018

Figure 4.7. Methane 25%

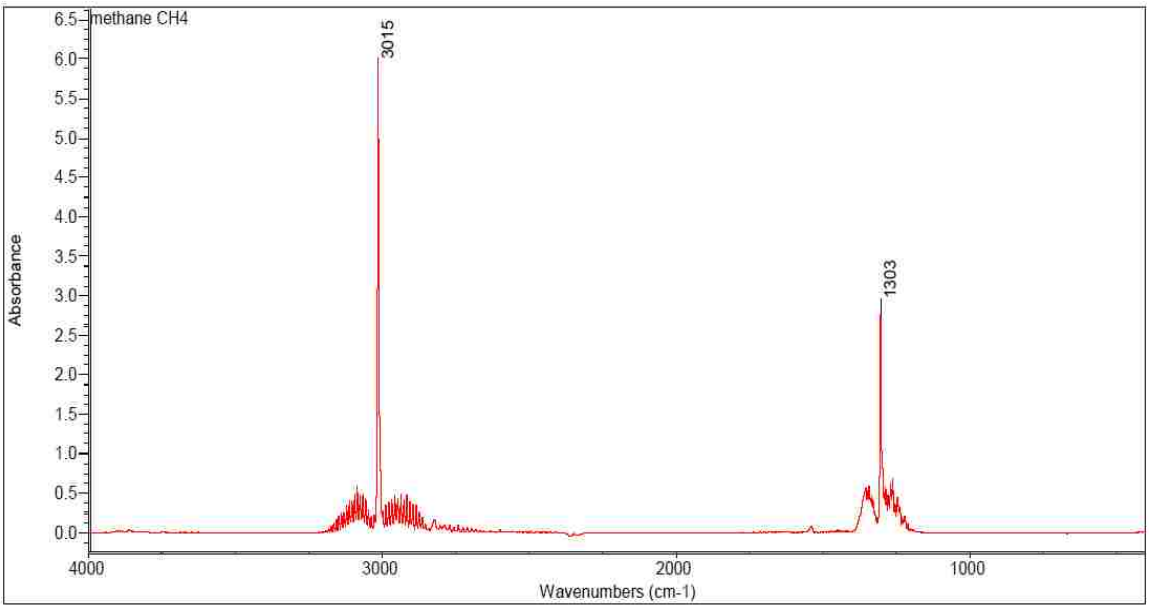

Tue Oct 10 11:56:38 2017
FIND PEAKS:
Spectrum: methane CH4
Region: 4000 400
Absolute threshold: 2.564
Sensitivity: 50
Peak list:

Position:	3015	Intensity:	6.414
Position:	1303	Intensity:	2.966

Figure 4.8. Methane 99.9%

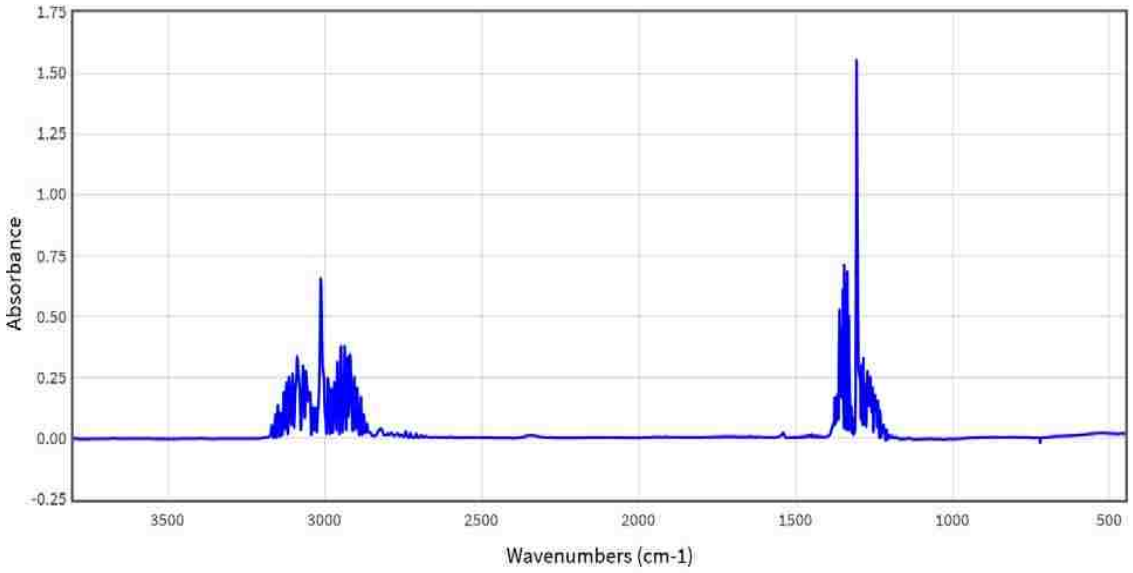

Figure 4.9. Methane NIST (references)

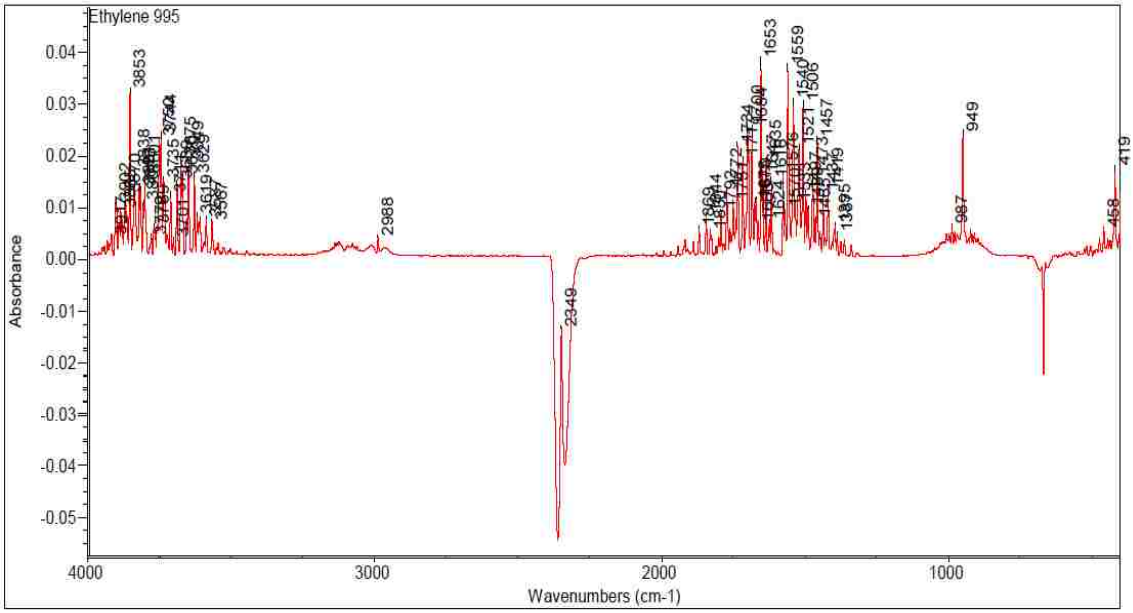

Tue Oct 10 11:45:39 2017
FIND PEAKS:
Spectrum: Ethylene 995
Region: 4000 400
Absolute threshold: -0.013
Sensitivity: 50
Peak list:

Position:	1653	Intensity:	0.0390
Position:	1559	Intensity:	0.0377
Position:	3853	Intensity:	0.0332
Position:	1506	Intensity:	0.0307
Position:	1540	Intensity:	0.0312
Position:	1684	Intensity:	0.0258
Position:	1700	Intensity:	0.0262

Figure 4.10 Ethylene 999ppm

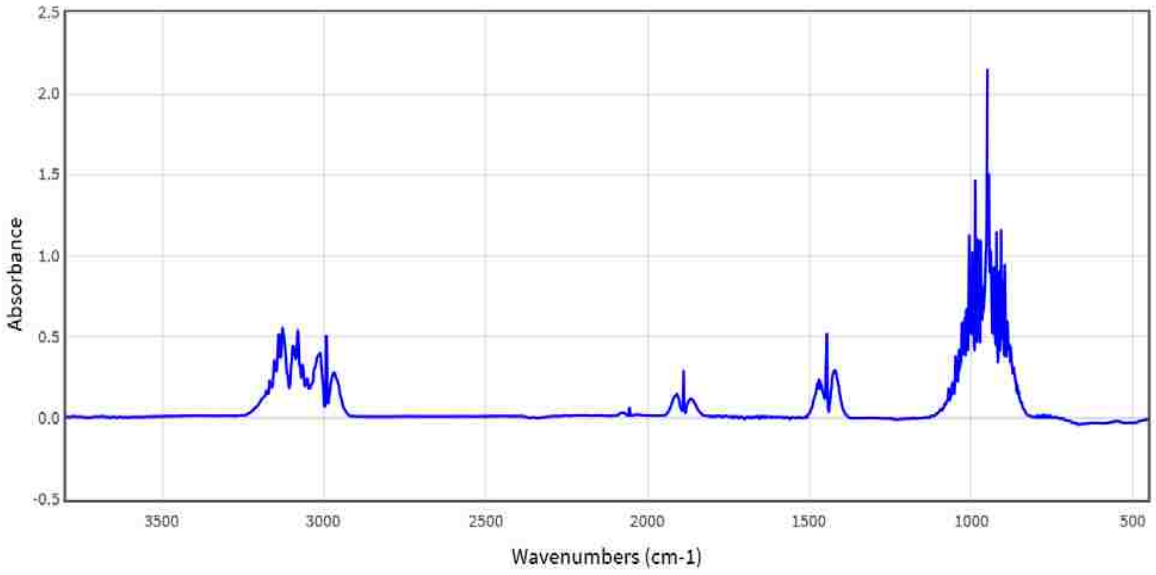

Figure 4.11. Ethylene NIST (reference)

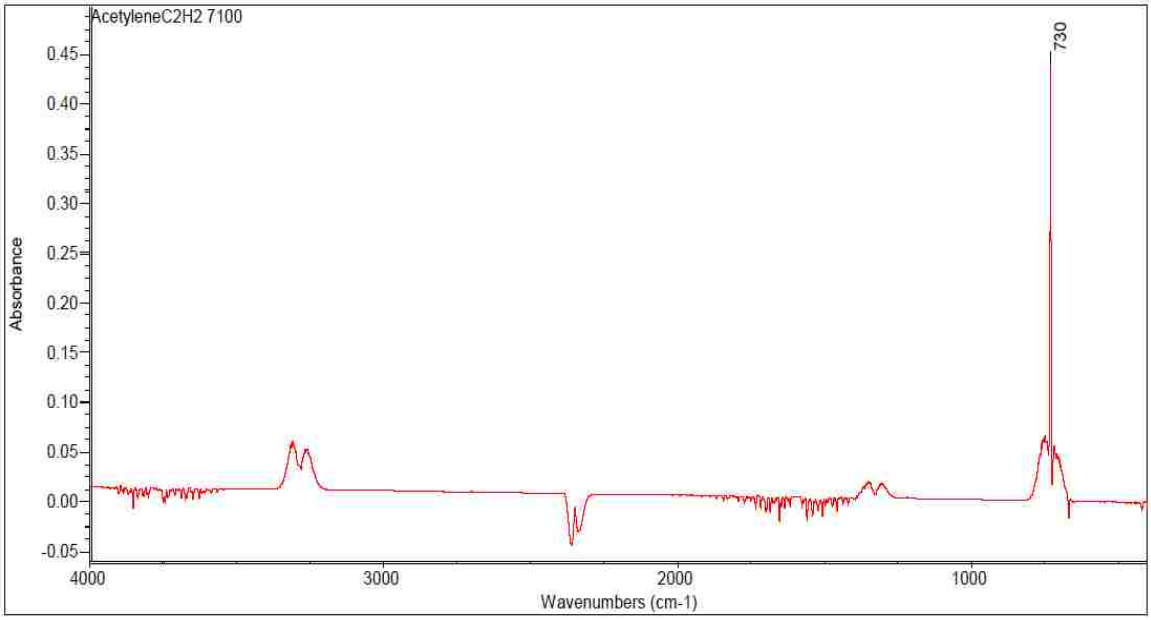

Figure 4.12. Acetylene 7100

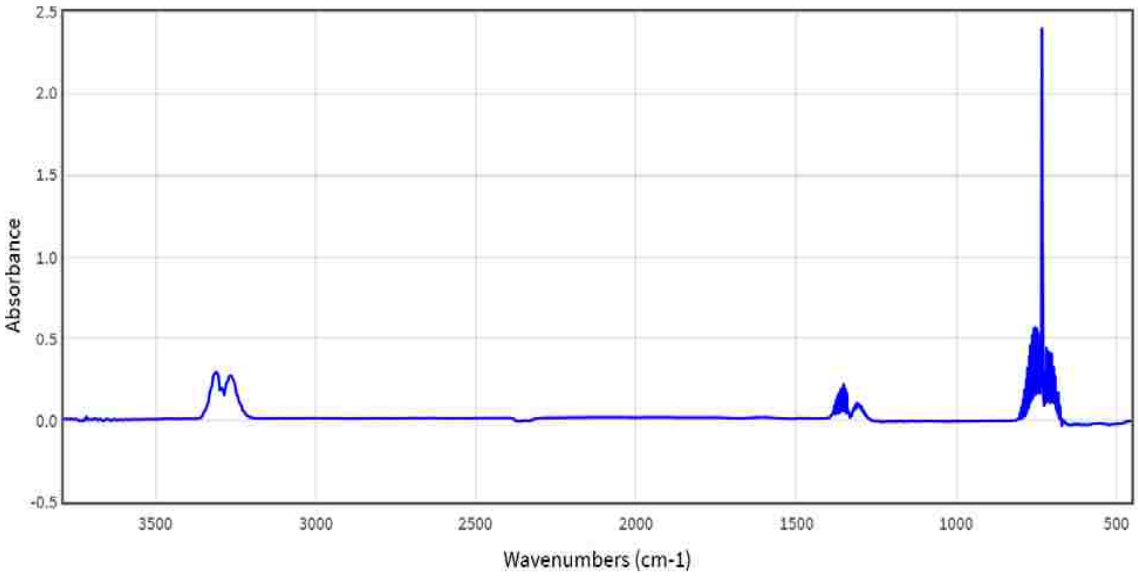

Figure 4.13 Acetylene NIST (reference)

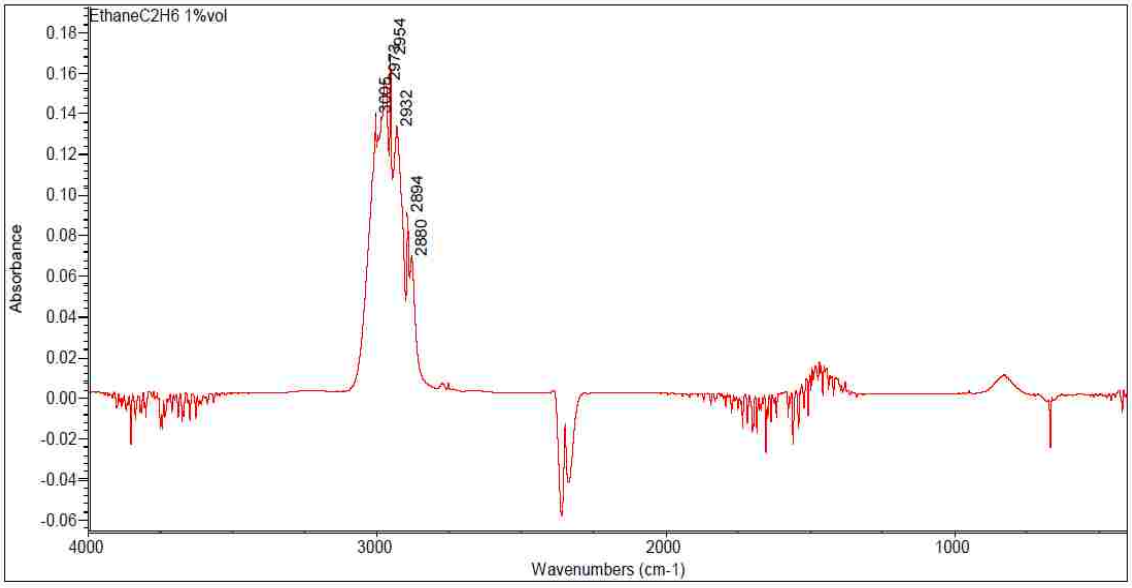

Tue Oct 10 11:09:33 2017
FIND PEAKS:
Spectrum: EthaneC2H6 1%vol
Region: 4000 400
Absolute threshold: 0.040
Sensitivity: 50
Peak list:

Position:	2954	Intensity:	0.169
Position:	2973	Intensity:	0.156
Position:	3005	Intensity:	0.140
Position:	2932	Intensity:	0.134
Position:	2894	Intensity:	0.0915
Position:	2880	Intensity:	0.0699

Figure 4.14. Ethane 1%

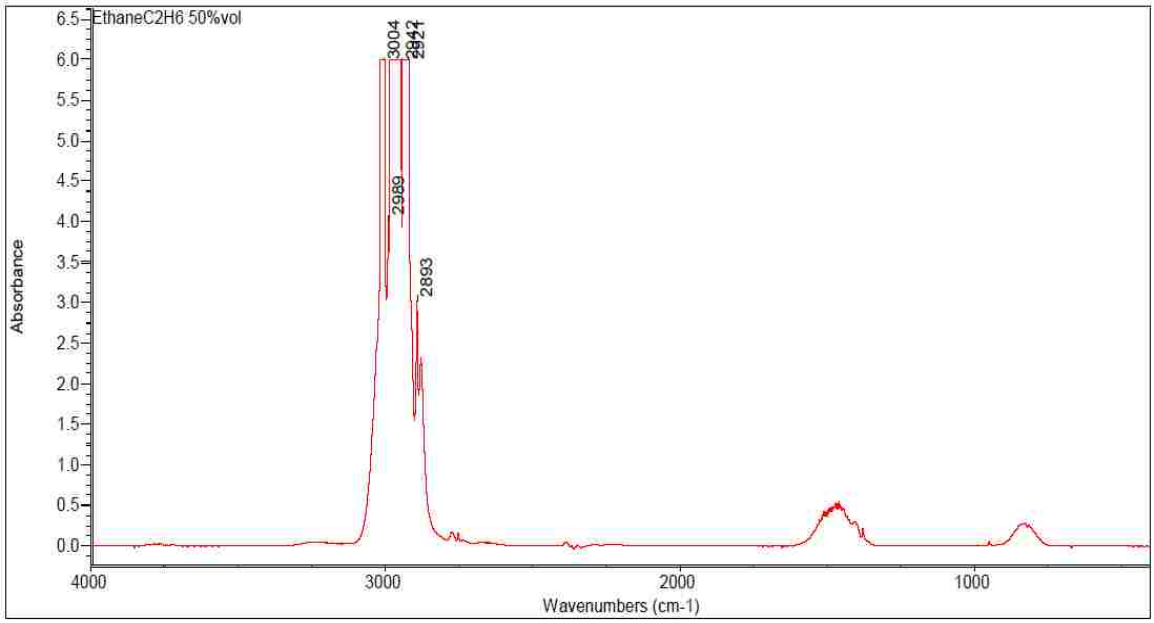

Tue Oct 10 11:29:53 2017
FIND PEAKS:
Spectrum: EthaneC2H6 50%vol
Region: 4000 400
Absolute threshold: 2.555
Sensitivity: 50
Peak list:

Position:	2921	Intensity:	6.299
Position:	2942	Intensity:	6.278
Position:	3004	Intensity:	6.321
Position:	2989	Intensity:	4.084
Position:	2893	Intensity:	3.074

Figure 4.15. Ethane 50%

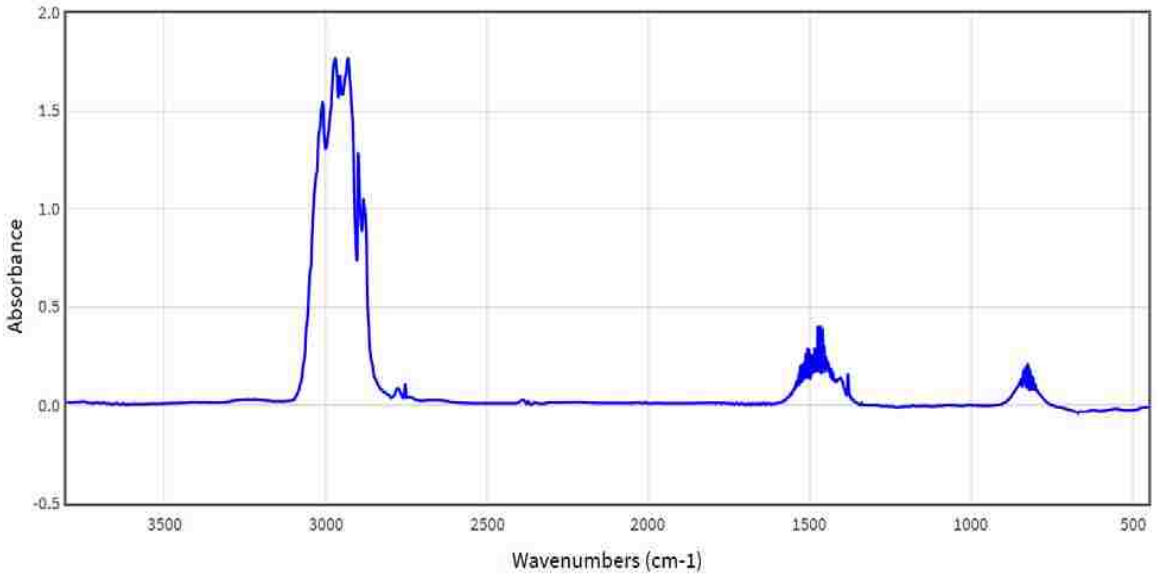

Figure 4.16 Ethane NIST (reference)

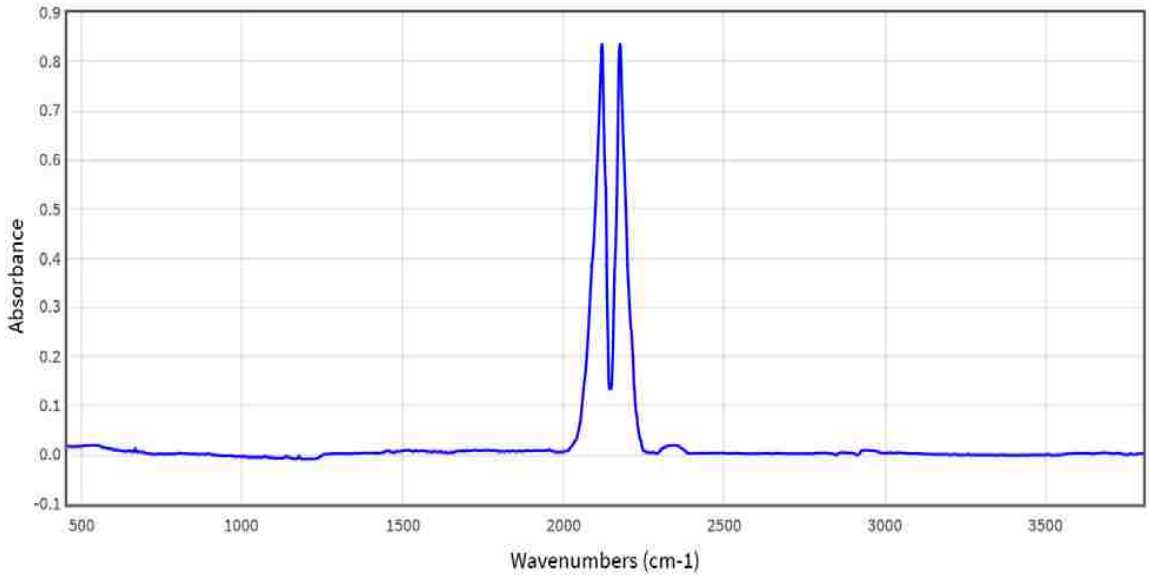

Figure 4.17. CO (reference)

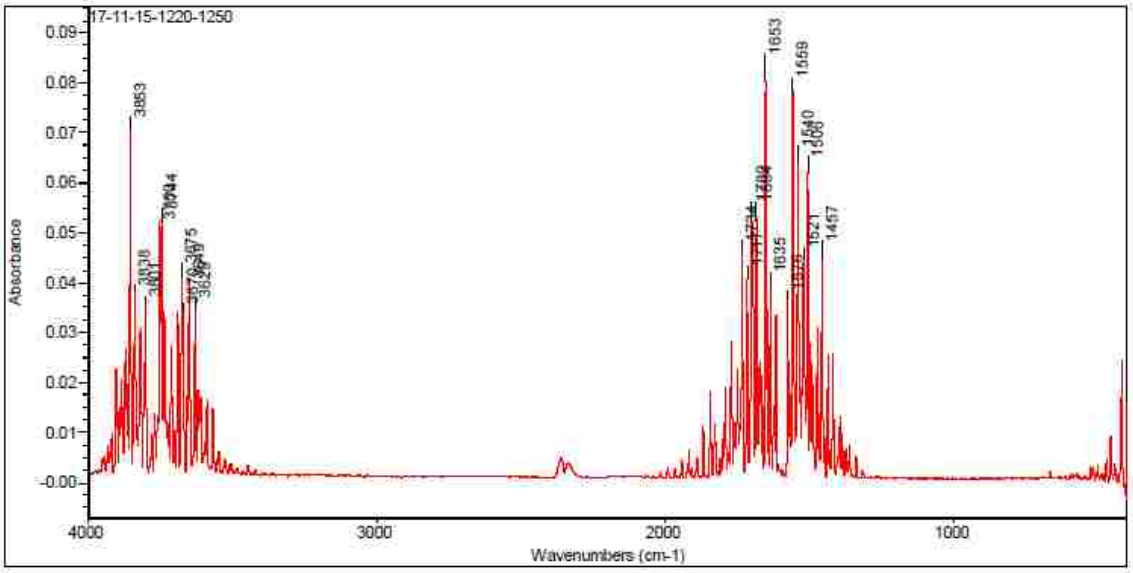

Figure 4.18. FTIR spectra result

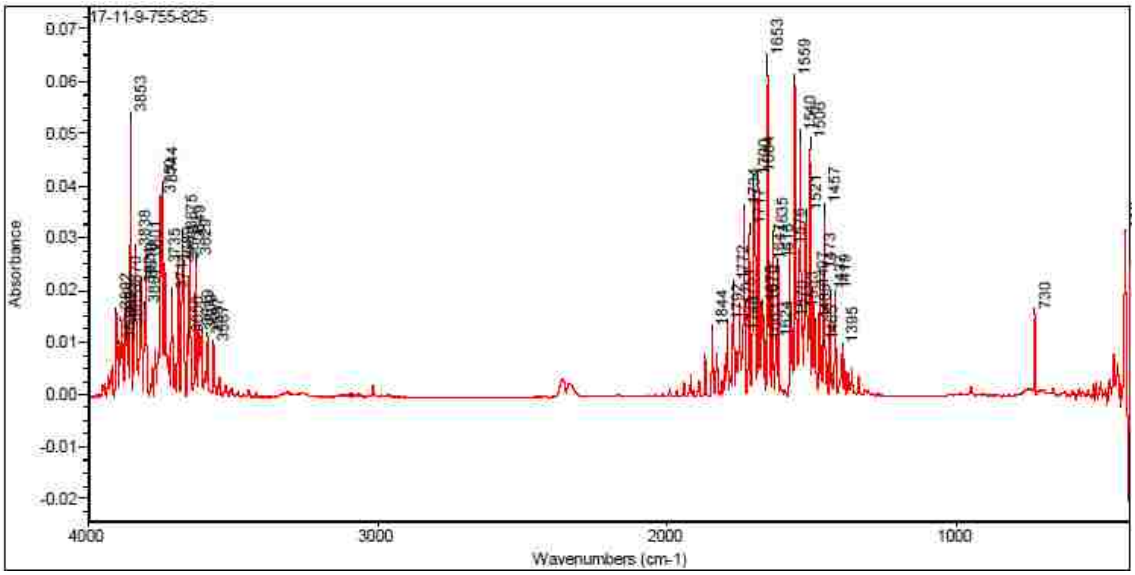

Figure 4.19. FTIR spectra

4.5.2. Detection Limits. These are the detection limits by the wavenumbers to the peaks for each gas.

Table 4. Wavenumbers limitation for different component

methane	3015	1304		
ethylene	419	949.94	1337-1869	3567-3917
ethane	2880-3006	1469.75		
acetylene	730	3259.69-3313.7		
CO	2100	2220		

4.5.3. The Qualitative and the Quantitative. For qualitative gas sample, we compared the spectra samples with the reference gases to match the positions of the sample peaks, and then we can recognize the gas in the sample. From a quantitative point of view, we calculates the composition of the gas in the sample by using the second

derivative method (to calculate the area under the curve) via Origin Pro 2017 software, which is called peak analyzer.

Table 5. FTIR results

Gases name	%Vol concentration
Ethylene (C2H4)	0.77-8.35
Acetylene(C2H2)	0.01-8.58
Methane(CH4)	0.1-2.1
Carbon Monoxide(CO)	14.5-32.7
N2,AR,H2(INERT GASES)	CANOT DETECTED BY FTIR

4.6. RESULTS ERROR

Many errors may occur (if any) in the results, such as in BET measurement after degassing when weighing the dry sample with the cell, where the sample is exposed to air and may have a little moisture. This will affect the amount of nitrogen adsorpted from the CB sample and could effect the surface area calculations. Also, in FTIR, the error in the results (if any) can happen from environmental effects, such as vapor water and CO_2, or human error when collecting the sample.

If the gas cell has any leak, is not clean or is not flashing, it probably contains an error. For gases tests, the error in the results (if any) can happen from the environmental effect which is the vapor water and CO_2. Moreover, for powder samples, the moisture environment may affect the accuracy.

It is worth mentioning that there are many other details that cannot be shown in this thesis for the privacy of the sponsoring company.

4.7. DISCUSSION

In this project, our goals to get high surface area for CB (main product) should be more than 80 m^2/gm by analyzing the powder for the samples, which is more than 60, via the BET technique.

BET measured the surface area, and from these results we can see the highest surface area is 40 m^2/gm, and the lowest one is 10 m^2/gm, and for the rest of the samples, the range of surface area values are from 25 to 35 m^2/gm. The data shows that there is no constant values for the surface area even with varying the flow rate of the feedstock and the reactor temperature. However, when we increased the bubbler temperature, the surface area decreased, due to an increase in the aromatic vapor amount that entered with feedstocks to the reactor.

Furthermore, our SEM images for four samples of the highest surface area show the particle shape is almost spheroidal, and also the results show there is a cluster (aggregate) in many zones.

From the literature review, there are four shape types of the CB particles (spheroidal, ellipsoidal, liner, and branched) and the spheroidal shape is observed in the thermal decomposition method, so, our SEM results are satisfied.

For the XRD test, we analyzed four samples. The results show that the CB is graphite material and the Lc ≈ 91.5 represents the crystal structure thickness in the c direction (Å), and d_{002} ≈ 3.46 represents distance between planes in the c direction (Å). This Lc number should be slightly smaller than the acceptable values because the thickness of the graphite unit cell is slightly larger than the standard. On the other hand, from the GC-analyzer, the gas analysis (side product) results show single peak after 4 min of the injection for all sixteen samples.

These results were compared with the reference gases methane and ethylene. The comparison shows that the reference gases' peak is observed at the same retention time, so, the single peak refers to one of them. Thus, the results from GC are not accurate because we expected more than one component from the reaction.

Therefore, we used FTIR to get more accurate results. Here we run more than 60 samples. All gas analysis results showed that the samples contain ethylene gas as a main product (in gases samples), and it appears in spectra of all the samples.

Also, acetylene gas and the small amount of unreacted methane both are displayed in our results. Furthermore, some of the gas samples contain carbon monoxide. These results appear when using oxygen gas with the feedstock. Also, there is an amount of AR, N_2, and H_2 that were not detected by GC or FTIR (inert gases).

At this moment of time, we could not reach the surface area that was expected to achieve the goals of this project because the heater was designed to reach approximately 2000^{o}C but it could not, because the resistance of the heating element was high.

Then, the heating element was replaced with a new one that has less resistance so it could let more current go through and raise the temperature. The heater reached to 1700^{o}C. All conditions were run at steady state at 1500^{o}C.

The project needs modification and extra work. This will be achieved with the company that designed this project to reach temperature more than 2000^{o}C and get high surface area for the CB product to achieve our goals.

5. REMARKS AND RECOMMENDATION

In this study, the results presented demonstrate the degree of information that can be achieved depending on the setup design and measurement techniques used. The experimental work carried out takes into account the different inlet feedstock concentration influences at varying operation conditions. Characterization of the carbon black, solid material (powder) and outlet gasses, was performed. The results demonstrate the necessary date to produce purist carbon black and also provide benchmarking data for computational fluid dynamics (CFD) simulation.

Futures studies will include continuous work on the project at a higher temperature (more than 2000ºC) and use of the computational fluid dynamics model (CFD) to validate the experimental data which obtained from this work for scale-up and large-scale design developments.

REFERENCES

A. Tomlinson E. Karakosta, M. Oakey, T.N. Danks, D.M. Heyes, S.E. Taylor, B Scherer et al. 2000. "General Information, What Is Carbon Black? - International Carbon Black Association - ICBA." *Carbon* 355(3): 5901–10.

Alcántara, Ricardo, Juan M. Jiménez-Mateos, Pedro Lavela, and José L. Tirado. 2001. "Carbon Black: A Promising Electrode Material for Sodium-Ion Batteries." *Electrochemistry Communications* 3(11): 639–42.

Anonymous. 2011. "Insights on Carbon Black Fundamentals."*Modern Dispersions, Incorporated(MDI)*.http://www.moderndispersions.com/CARBON_20BLACK_20FUNDAMENTALS.pdf. ASTM. 1990. Annual Book of ASTM Standards *ASTM D1298 - 85*.

ASTM International. 2012. D6556 ASTM International *Standard Test Method for Carbon Black — Total and External Surface Area by Nitrogen*. http://www.biochar-international.org/sites/default/files/ASTM D6556-10 N2 BET for Carbon Black .juhu2739.pdf.

Bernal, M, I Nenadic, M W Urban, and J F Greenleaf. 2011. "Material Property Estimation for Tubes and Arteries Using Ultrasound Radiation Force and Analysis of Propagating Modes." *Journal of the Acoustical Society of America* 129(3): 1344–54.

Biscoe, J., and B. E. Warren. 1942. "An X-Ray Study of Carbon Black." *Journal of Applied Physics* 13(6): 364–71.

Black, Shawinigan Acetylene, Black Pearls, and Royal Spectra. 1996. "Carbon Black." *IARCmonograph*1995(April1984):43..88.http://monographs.iarc.fr/ENG/Monographs/vol93/mono93-6.pdf.

Borah, Dipu, Shigeo Satokawa, Shigeru Kato, and Toshinori Kojima. 2008. "Characterization of Chemically Modified Carbon Black for Sorption Application." *Applied Surface Science* 254(10): 3049–56.

Borchard, Nils et al. 2014. "Black Carbon and Soil Properties at Historical Charcoal Production Sites in Germany." *Geoderma* 232–234: 236–42.

Bossuyt, Heleen, Johan Six, and Paul F. Hendrix. 2006. "Interactive Effects of Functionally Different Earthworm Species on Aggregation and Incorporation and Decomposition of Newly Added Residue Carbon." *Geoderma* 130(1–2): 14–25.

Brunauer, Stephen, P. H. Emmett, and Edward Teller. 1938. "Adsorption of Gases in Multimolecular Layers." *Journal of the American Chemical Society* 60(2): 309–19.

Carbon, Black, and Climate Change. 2010. "What Is Black Carbon?" *Center for Climate and Energy Solutions* (April): 3.

Chen, Hongmei et al. 2014. "Production of Black Carbon-like and Aliphatic Molecules from Terrestrial Dissolved Organic Matter in the Presence of Sunlight and Iron." *Environmental Science and Technology Letters* 1(10): 399–404.

Dong, Pengwei et al. 2017. "Chemically Treated Carbon Black Waste and Its Potential Applications." *Journal of Hazardous Materials* 321: 62–72.

Donnet, J-B. 1993. "Carbon Black: Science and Technology, Second Edition." : 461.

Donnet, Jean-Baptiste, Roop Chand Bansal, and Meng-Jiao Wang. 1993. 1995 IARC Monographs on the Evaluation of Carcinogenic Risks to Humans *Carbon Black: Science and Technology*. New York United States.

Dons, Evi et al. 2012. "Personal Exposure to Black Carbon in Transport Microenvironments." *Atmospheric Environment* 55: 392–98.

DuBay, Shane G., and Carl C. Fuldner. 2017. "Bird Specimens Track 135 Years of Atmospheric Black Carbon and Environmental Policy." *Proceedings of the National AcademyofSciences*:201710239.http://www.pnas.org/lookup/doi/10.1073/pnas.1710239114.

Endter, F. and Gebauer, H. 1956. "Elektronenmikroskopischen Aufnahmen." *Optik* 13: 97.

Fan, Xiaodan, and Xiangkai Zhang. 2008. "Adsorption Properties of Activated Carbon from Sewage Sludge to Alkaline-Black." *Materials Letters* 62(10–11): 1704–6.

Fowles, Malcolm. 2007. "Black Carbon Sequestration as an Alternative to Bioenergy." *Biomass and Bioenergy* 31(6): 426–32.

Galli, Giulia. 2010. "Computer-Based Modeling of Novel Carbon Systems and Their Properties." 3: 37–57. http://link.springer.com/10.1007/978-1-4020-9718-8.

Geschke, D. 2007. 199 Zeitschrift für Physikalische Chemie *Physical Properties of Polymers Handbook*.

Golberg, E.D. 1985. 244 Journal of the American Veterinary Medical Association *Black Carbon in the Environment*. Goldstein, Joseph et al. 2003. 44 Scanning Electron Microscopy and Xray Microanalysis *Scanning Electron Microscopy and X-Ray Microanalysis*.

Gómez-Serrano, V, C.M González-García, and M.L González-Martín. 2001. "Nitrogen Adsorption Isotherms on Carbonaceous Materials. Comparison of BET and Langmuir Surface Areas." *Powder Technology* 116(1): 103–8.

Griffiths, Peter R, and James A. De Haseth. 2007. Chemical Analysis: A Series of Monographs on Analytical Chemistr and Its Applications *Fourier Transform Infrared Spectrometry*.

Haiqing Liu. 2016. “Designing Functional Nanocomposites towards Energy Applications: Examining the Performance of Hierarchical Nanostructures as a Function of Composition, Morphology, and Structure for Fuel Cell and Photovoltaic Device Applications.” stony Brook University.

J. B. Donnet, R. C. Bansal, M. J. Wang (eds). 1993. *Carbon Black: Science and Technology*. Marcel Decker, New York Hongkong.

James E. Mark. 2007. *Physical Properties of Polymers Handbook*. second edi.

Jianfeng ZHANG, Rong TU, Takashi GOTO. 2013. “Precipitation of Ni and NiO Nanoparticle Catalysts on Zeolite and Mesoporous Silica by Rotary Chemical Vapor Deposition.” *Journal of the Ceramic Society of Japan* 121(1418): 891–94.

Kim, J.-H., and H.-Y. Jeong. 2005. “A Study on the Material Properties and Fatigue Life of Natural Rubber with Different Carbon Blacks.” *International Journal of Fatigue* 27(3): 263–72.

Knoblauch, Christian, Arina-Ann Maarifat, Eva-Maria Pfeiffer, and Stephan M. Haefele. 2011. “Degradability of Black Carbon and Its Impact on Trace Gas Fluxes and Carbon Turnover in Paddy Soils.” *Soil Biology and Biochemistry* 43(9): 1768–78.

Köchling, K. H., B. McEnaney, S. Müller, and E. Fitzer. 1985. “International Committee for Characterization and Terminology of Carbon ‘first Publication of 14 Further Tentative Definitions.’” *Carbon* 23(5): 601–3.

Kraus, Gerard. 1978. “Reinforcement of Elastomers by Carbon Black.” *Rubber Chemistry and Technology* 51(2): 297–321.

Kuhlbusch, Thomas A. J. 1998. “Black Carbon and the Carbon Cycle.” *Science* 280(5371): 1903–4.

Kwon, W, J M Kim, and S W Rhee. 2013. “Electrocatalytic Carbonaceous Materials for Counter Electrodes in Dye-Sensitized Solar Cells.” *Journal of Materials Chemistry A* 1(10): 3202–15.

Liang, L. 2004. “Recovery and Evaluation of the Solid Products Produced by Thermocatalytic Decomposition of Tire Rubber Compounds. PhD Thesis.”

Lohmann, R., J. K. Macfarlane, and P. M. Gschwend. 2005. “Importance of Black Carbon to Sorption of Native PAHs, PCBs, and PCDDs in Boston and New York Harbor Sediments.” *Environmental Science and Technology* 39(1): 141–48.

Loutfy, Rafik O. 1986. “Electrochemical Characterization of Carbon Black.” *Carbon* 24(2): 127–30.

Major, Julie, Johannes Lehmann, Marco Rondon, and Christine Goodale. 2010. "Fate of Soil-Applied Black Carbon: Downward Migration, Leaching and Soil Respiration." *Global Change Biology* 16(4): 1366–79.

Martínez, J D, R Murillo, and T García. 2013. "Production of Carbon Black from the Waste Tires Pyrolysis." *Bol. Grupo Español Carbón* (i): 10–14.

Mattson, David R. 1978. "SENSITIVITY OF A FOURIER TRANSFORM INFRARED SPECTROMETER." *Applied Spectroscopy* 32(4): 335–38.

Medalia, A. I. 1978. "Effect of Carbon Black on Dynamic Properties of Rubber Vulcanizates." *Rubber Chemistry and Technology* 51(3): 437–523.

Medalia, A. I., and F. A. Heckman. 1969. "Morphology of aggregates—II. Size and Shape Factors of Carbon Black Aggregates from Electron Microscopy." *Carbon* 7(5): 567–82.http://www.sciencedirect.com/science/article/pii/0008622369900293%0Ahttp://www.sciencedirect.com/science/article/pii/0008622369900293/pdf?md5=5838ccb53b332c993379493209b8acfb&pid=1-s2.0-0008622369900293-main.pdf.

Medalia, Avrom I. 1986. "Electrical Conduction in Carbon Black Composites." *Rubber Chemistry and Technology* 59: 432–54.

Miao, Xiaohuan et al. 2013. "Highly Crystalline Graphene/carbon Black Composite Counter Electrodes with Controllable Content: Synthesis, Characterization and Application in Dye-Sensitized Solar Cells." *Electrochimica Acta* 96: 155–63.

Moulin, L. et al. 2017. "Assessment of Recovered Carbon Black Obtained by Waste Tires Steam Water Thermolysis: An Industrial Application." *Waste and Biomass Valorization* 8(8): 2757–70.

Payne, A. R., and R. E. Whittaker. 1970. "Reinforcement of Rubber with Carbon Black." *Composites* 1(4): 203–14.

Pierson, Hugh O. 1993. *HANDBOOK OF CARBON , GRAPHITE , DIAMOND AND FULLERENES by*.

Poudel, Prashant, and Qiquan Qiao. 2014. "Carbon Nanostructure Counter Electrodes for Low Cost and Stable Dye-Sensitized Solar Cells." *Nano Energy* 4: 157–75.

Probst, Nicolaus, and Eusebiu Grivei. 2002a. "Structure and Electrical Properties of Carbon Black." *Carbon* 40(2): 201–5.

Pundlik, Ware, Shukla Vikaskumar, Kushvah Avadhesh, and Desai K. R. 2013. "Acid Demineralization and Characterization of Carbon Black Obtained From Pyrolysis ofWaste Tyre Using Thermal Shock Process." *International Journal of Research in Chemistry and Environment* 3(1): 208–12.

Rating, Visual Dispersion. 2000. "Standard Test Methods for Carbon Black — Dispersion in Rubber 1." *Test* 9(Reapproved): 1–6.

La Rosa, J Rivera-De et al. 2007. "Natural Zeolites Used as Surface Reaction for Phthalocyanine Synthesis." *Materials and Manufacturing Processes* 22(3): 314–17.

Samaržija-Jovanović, Suzana, Vojislav Jovanović, Gordana Marković, and Milena Marinović-Cincović. 2009. "The Effect of Different Types of Carbon Blacks on the Rheological and Thermal Properties of Acrylonitrile Butadiene Rubber." *Journal of Thermal Analysis and Calorimetry* 98(1): 275.

Schubert, B., Ford, F. P. and Lyon, F. 1969. "Encyclopedia of Industrial Chemical Analysis." 8.

Snowdon, Michael R., Amar K. Mohanty, and Manjusri Misra. 2014. "A Study of Carbonized Lignin as an Alternative to Carbon Black." *ACS Sustainable Chemistry and Engineering* 2(5): 1257–63.

Sorahan, Tom et al. 2001. "A Cohort Mortality Study of U.K. Carbon Black Workers, 1951-1996." *American Journal of Industrial Medicine* 39(2): 158–70.

Sweitzer, C. W. and Goodrich, W. C. 1944. "Rubber Age." : 469.

Syvitski, J P M, K W G LeBlanc, and K W Asprey. 1991. "Interlaboratory, Interinstrument Calibration Experiment." *Principles, methods, and application of particle size analysis*: 174–94.

Syvitski J. P. M. 1991. *Principles, Methods, and Application of Particle Size Analysis*. Cambridge, New York, Port Chester, Melbourne, Sydney: Cambridge University.

Szozda, Ryszard. 1996. "Pneumoconiosis in Carbon Black Workers." *Journal of UOEH* 18(3): 223–28.

Tang, Qunwei et al. 2015. "Recent Advances in Alloy Counter Electrodes for Dye-Sensitized Solar Cells. A Critical Review." *Electrochimica Acta* 178: 886–99.

Tomasini, Eugenia P. et al. 2012. "Micro-Raman Spectroscopy of Carbon-Based Black Pigments." In *Journal of Raman Spectroscopy*, , 1671–75.

Wang, Lili et al. 2011. "Preparation of Carbon Black from Rice Husk by Hydrolysis, Carbonization and Pyrolysis." *Bioresource Technology* 102(17): 8220–24.

Wang, Meng-Jiao et al. 2003. “Carbon Black.” In Kirk-Othmer Encyclopedia of Chemical Technology.

Wójtowicz, Marek A, Rosemary Bassilakis, and Michael A Serio. 2004. “Carbon Black Derived from Waste Tire Pyrolysis Oil.” *Advanced Fuel Research, Inc.* (October): 1–7.

Zielinski, T., and J. Kijenski. 2005. “Plasma Carbon Black - The New Active Additive for Plastics.” *Composites Part A: Applied Science and Manufacturing* 36(4): 467–71.

VITA

Shadha Khalid Jebur was born in Baghdad, Iraq, 1986. She received his B.S. in Chemical Engineering from the University of Technology Baghdad, Iraq in 2008. Before joining Missouri University of Science and Technology (Missouri S&T), Shadha worked as an operator engineering and controlling in an oil refinery in Baghdad for three and a half years, and she received many awards and certificates while she was in this position.

Shadha started at Missouri S&T during the spring semester of 2017 to work under the supervision of Dr. Joseph Smith. She received her Master Degree in Chemical Engineering from Missouri S&T in May 2018.